Interaction point estimation and beam parameter variations in DELPHI with the VSAT

August 26, 1995

Christina Jarlskog
Lund University
Sweden

Abstract

The beam parameter variations during 1994 data taking, obtained by the measurements of the Very Small Angle Tagger (VSAT) luminometer, are presented; a comparison of the 1993 and 1994 data with the corresponding 1994 measurements obtained by the Micro Vertex Detector (VD) and the Time Projection Chamber (TPC) is shown.

Contents

1   Introduction

The Very Small Angle Tagger (VSAT) is an electromagnetic sampling calorimeter for the luminosity measurement in DELPHI. It consists of four rectangular modules placed symmetrically at about 7.7 m from the DELPHI origin, around a short elliptical section of the beam pipe downstream the low beta superconducting quadrupoles (SCQ) as shown in fig. 1. The distance between two neighbouring modules is about 12 cm, corresponding to the smaller beam pipe dimension in that region. Since the physical process studied for the luminosity measurement is Bhabha scattering [1], where electrons and positrons are emitted back to back, we use the coincidences of signals between a module in the forward region and a module in the backward region, thus defining two diagonals for the trigger: diagonal 1 (modules F1-B2) and diagonal 2 (modules F2-B1).
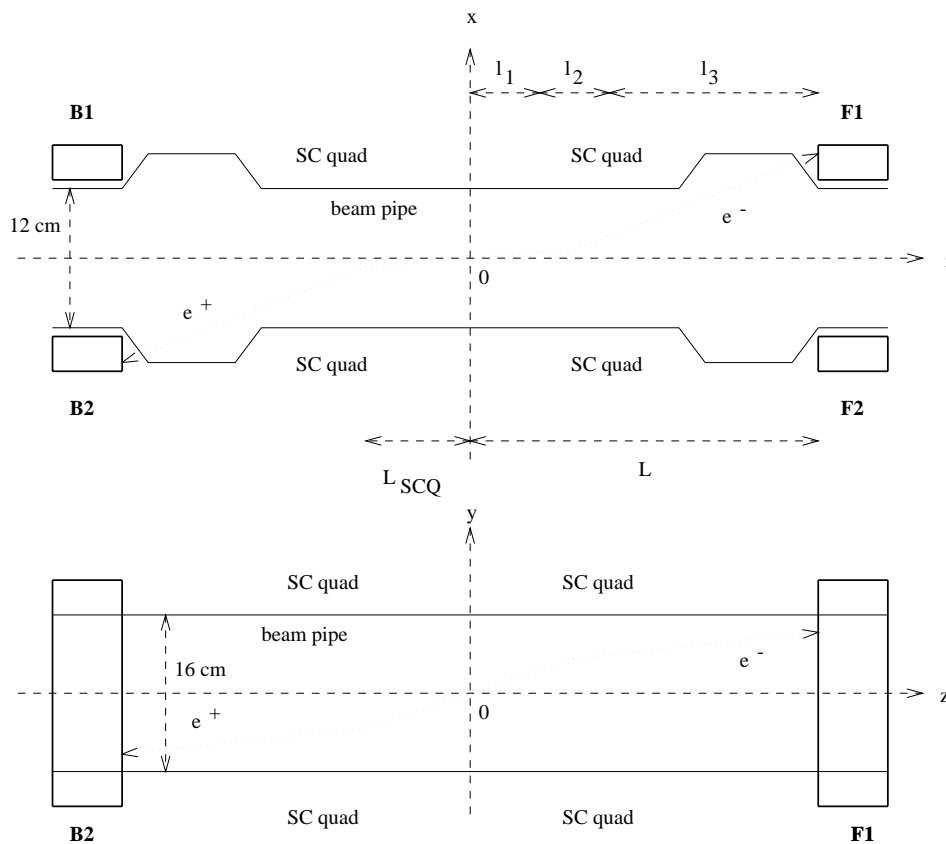

Figure 1: *Layout of the position of the VSAT modules in the (x,z) and (y,z) planes: the distance L_{SCQ} of the center of the superconducting quadrupoles from the DELPHI origin is about 4 m and the distance L of the front of the VSAT modules is about 7.7 m.*

Each VSAT module [2, 3, 4] contains 12 tungsten absorbers ($X_0 = 0.38$ cm) interspaced with 12 silicon planes (Full Area Detectors, (FAD)) for energy measurement (fig. 2). The dimensions of the calorimeters are 3 cm in the transverse horizontal direction (x), 5 cm in the vertical direction (y) and 24 radiation lengths (about 10 cm) along the beam direction (z). The center of the electromagnetic shower is given by three silicon strip planes with

1 mm pitch placed close to the shower maximum at 5, 7 and 9 r.l.; the second plane is used for the y coordinate measurement and the other two planes for the x coordinate measurement. The angular acceptance of a module is 5-7 mrad in polar angle and $\pm$ 50 degrees in azimuth.

Figure 2: *Layout of the VSAT modules.*

Due to the very small emission angle of the Bhabha events accepted in the VSAT, the accepted Bhabha cross section is very large (about 500 nb). This allows to monitor with high statistics, besides the luminosity, also the beam background and the variation of beam parameters.

In this paper we will discuss the monitoring of the beam parameters, which is an important task for different reasons.

The first reason is the online cross check of similar measurements done by the general monitoring system of LEP at the DELPHI interaction point. These measurements are used in order to optimize the luminosity, which depends strongly on the beam parameters. Among the DELPHI detectors, the VSAT has the highest accepted cross section and can thus collect sufficient statistics in a time interval ($\approx$ 10 minutes) relevant for online control. As will be shown in the following, even though the VSAT data do not allow to monitor the variations of each beam parameter separately, they provide useful information on combined variations.

The second reason is the offline estimation of variation of beam parameters. This information is used at different levels in the analysis of DELPHI events. For example, the variations of the beamspot position as well as those of the directions of the incident particles are used to optimize the alignment of the different DELPHI detectors. Furthermore, when it comes to the luminosity measurement done by the VSAT, the beam parameter monitoring provides an important cross check: the Bhabha cross section in the VSAT acceptance depends on the beam parameters and consequently, it has to be corrected for their variations. Fortunately, as shown in [3], such corrections can be done with a high

level of accuracy (better than .1%) by using directly quantities measured by the VSAT without any need to know in detail the values of the beam parameters themselves. However, since the correction function is determined by an extensive simulation of different beam conditions done by a fast Monte Carlo program (FASTSIM), it is important to cross check the validity of the model used in FASTSIM by comparing the description of the variations of the beam parameters that we obtain from VSAT data with data from LEP or other DELPHI detectors.

The effect of the variation of beam parameters on the quantites measured by the VSAT will be discussed in section 2. In section 3, the procedure used to obtain the information on the beam parameters from VSAT measurement will be described, as well as a comparison with the values measured by the VD and by the TPC. In section 4, the variation of the beam parameters during 1994 will be discussed.

2   Beam parameters monitoring with the VSAT

The beam parameters that are relevant for the following discussion are:

- the average values of the coordinates x_b, y_b and z_b of the interaction point;

- the corresponding beam widths σ_x, σ_y and σ_z;

- the average values of the incident positron and electron beam angles at the interaction point, in the (x, z) and in the (y, z) planes (we will call them briefly *tilts*), respectively θ_+^x, θ_-^x, θ_+^y and θ_-^y;

- the beam divergence in the two planes, that is the spread around the above average angles.

The quantities measured with the VSAT which are used to extract information on the beam parameters are the x and y coordinates of the impact points of the scattered leptons in the four modules; the angles of the outgoing particles cannot be measured, which disqualifies the detector for monitoring all the above mentioned parameters. However, we can extract information on most of the beam parameters by combining the VSAT data with the measurements of the coordinates of the interaction point done by the VD and TPC, as will be discussed in section 3. In this section, we will discuss the dependence on the beam parameters of the variables measured by the VSAT.

2.1   Beam parameters in the (x,z) plane

Figure 3 shows two Bhabha events in the (x,z) plane in the diagonals of the detector for the ideal situation in which the interaction point coincides with the nominal position $(x_b = y_b = z_b = 0)$. We have assumed that the trajectories of the incoming particles are along the z-axis, so we also have zero beam tilts. In order to be able to represent the trajectories of the scattered particles as straight lines, we take into account the divergent effect of the superconducting quadrupoles (in first approximation) by moving the modules to an effective distance, l_x=12.6 m, which is assumed to be the same for all modules. The production angle of the Bhabha pair in diagonal i is denoted by θ_i^x and is defined to be
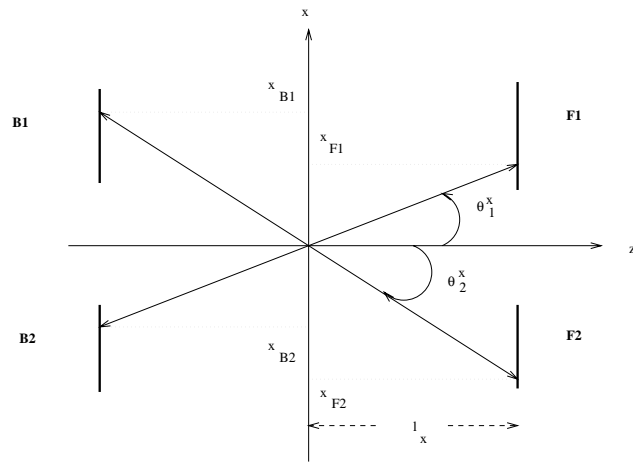
Figure 3: *Events on the two diagonals for zero beam displacement and zero tilts.*

always positive. Since those angles are very small we can calculate the x coordinates of the impact points of the particles on the modules as follows:

$$x_{F1} = l_x \theta_1^x \qquad x_{B2} = -l_x \theta_1^x$$

$$x_{B1} = l_x \theta_2^x \qquad x_{F2} = -l_x \theta_2^x$$

(1)

However, this ideal condition is rarely the case, since the beams do not usually cross at the nominal position. Fig. 4 represents a more realistic situation, in which we have included a nonzero beam displacement in the x direction, x_b. The constant f_x is the amplification factor of the particle trajectories due to the superconducting quadrupoles. It is of the order of 2.1 for the currents of the quadrupoles used during both 1993 and 1994 data taking and it is practically the same for all four modules. The emission angles are the
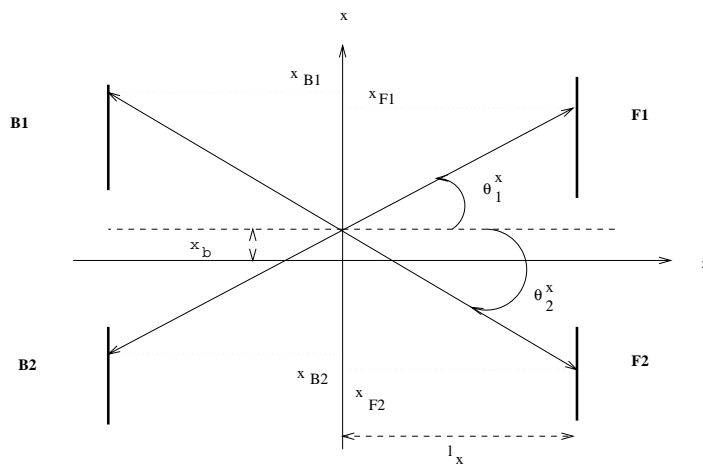
Figure 4: *Events on the two diagonals for zero z displacement and zero tilts.*

same as in fig. 3, but the x coordinates of the impact points are now given by

$$x_{F1} = f_x x_b + l_x \theta_1^x \qquad x_{B2} = f_x x_b - l_x \theta_1^x$$

$$x_{B1} = f_x x_b + l_x \theta_2^x \qquad x_{F2} = f_x x_b - l_x \theta_2^x \tag{2}$$

The next step is to see how the impact points will be affected by a beam displacement in the z direction. We will therefore include a shift of the interaction point equal to z_b, as shown in fig. 5. As evident from fig. 5, the effect of the z displacement is equivalent
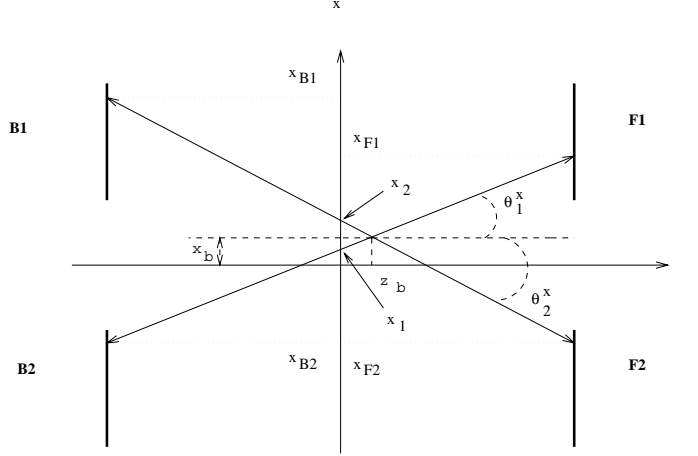
Figure 5: *Events on the two diagonals for nonzero beam displacements, x_b and z_b, and zero tilts.*

to that of two different x displacements, x_1 and x_2, in the two diagonals taken at z=0:

$$x_1 = x_b - z_b \theta_1^x \qquad x_2 = x_b + z_b \theta_2^x. \tag{3}$$

The impact points are thus given by

$$x_{F1} = f_x(x_b - z_b \theta_1^x) + l_x \theta_1^x \qquad x_{B2} = f_x(x_b - z_b \theta_1^x) - l_x \theta_1^x$$

$$x_{B1} = f_x(x_b + z_b \theta_2^x) + l_x \theta_2^x \qquad x_{F2} = f_x(x_b + z_b \theta_2^x) - l_x \theta_2^x. \tag{4}$$

We can now consider the case of nonzero tilts. Fig. 6 shows events in the two diagonals, where it has been assumed that the positron beam has a positive tilt, θ_+^x, whereas the electron beam has a negative tilt, θ_-^x. The equations for the x impact points will now be affected in terms of the production angle, namely

$$x_{F1} = f_x x_b + l_x(\theta_1^x - |\theta_-^x|) = f_x x_b + l_x(\theta_1^x + \theta_-^x) \quad x_{B2} = f_x x_b - l_x(\theta_1^x + |\theta_+^x|) = f_x x_b - l_x(\theta_1^x + \theta_+^x)$$

$$\tag{5}$$

$$x_{B1} = f_x x_b + l_x(\theta_2^x - |\theta_+^x|) = f_x x_b + l_x(\theta_2^x - \theta_+^x) \quad x_{F2} = f_x x_b - l_x(\theta_2^x + |\theta_-^x|) = f_x x_b - l_x(\theta_2^x - \theta_-^x)$$

If we combine eqs. (4) and (5), we obtain for the general case of nonzero beam displacements and nonzero tilts:

$$x_{F1} = f_x(x_b - z_b(\theta_1^x + \theta_-^x)) + l_x(\theta_1^x + \theta_-^x) \qquad x_{B2} = f_x(x_b - z_b(\theta_1^x + \theta_+^x)) - l_x(\theta_1^x + \theta_+^x)$$

$$(6)$$

$$x_{B1} = f_x(x_b + z_b(\theta_2^x - \theta_+^x)) + l_x(\theta_2^x - \theta_+^x) \qquad x_{F2} = f_x(x_b + z_b(\theta_2^x - \theta_-^x)) - l_x(\theta_2^x - \theta_-^x)$$
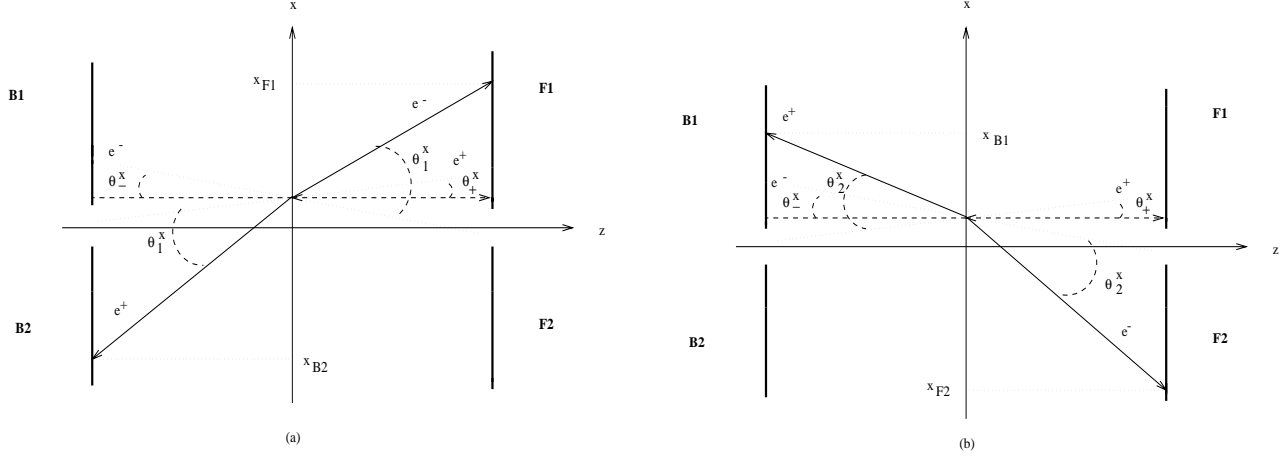

Figure 6: *Events for zero z displacement and nonzero tilts (a) on diagonal 1 and (b) on diagonal 2.*

From these equations, we see that it is convenient to define the following quantities:

$$\Delta x_1 = x_{F1} + x_{B2} = 2 \cdot f_x(x_b - z_b(\theta_1^x + \theta_x)) + \epsilon_x l_x$$

$$(7)$$

$$\Delta x_2 = x_{F2} + x_{B1} = 2 \cdot f_x(x_b + z_b(\theta_2^x - \theta_x)) + \epsilon_x l_x$$

where we have defined the average tilt, θ_x, and the acollinearity, ϵ_x, as follows

$$\theta_x = \frac{\theta_+^x + \theta_-^x}{2} \qquad \epsilon_x = \theta_-^x - \theta_+^x \qquad (8)$$

To better separate the dependence on different beam parameters, we define the following quantities:

$$\Delta x_0 = \frac{\Delta x_1 + \Delta x_2}{2} = 2 \cdot f_x x_b + \epsilon_x l_x + f_x z_b(\theta_2^x - \theta_1^x - 2\theta_x) \qquad (9)$$

$$\delta x = \Delta x_2 - \Delta x_1 = 2 \cdot f_x z_b(\theta_1^x + \theta_2^x) \qquad (10)$$

By taking the average over a reasonably long period of time (for this analysis, it is useful to use the time needed to write a cassette, which is about 20 minutes and corresponds to about 4 K events), we can substitute θ_1^x and θ_2^x with their average values, which are both very close to 5.5 mrad. This shows that δx essentially depends only on the value of z_b. On the contrary, Δx_0 essentially measures the combined effect of the beam x displacement and beam acollinearity in the (x,z) plane, since the third term in eq. (9) is completely negligible.

The similarity of the x_b and ϵ_x effects on the impact points is clearly depicted in fig. 7, where we have assumed for simplicity that only the electron beam has a nonzero tilt: the full lines correspond to outgoing particle tracks for $x_b = \theta^x_- = \theta^x_+ = 0$, whereas the dotted line shows the case of nonzero acollinearity and x_b=0 and the dashed line shows an event with zero acollinearity but nonzero x_b, which has the same impact points on the modules, showing that the ϵ_x and x_b effects are equivalent, and therefore these two parameters cannot be determined separately using the VSAT information alone.
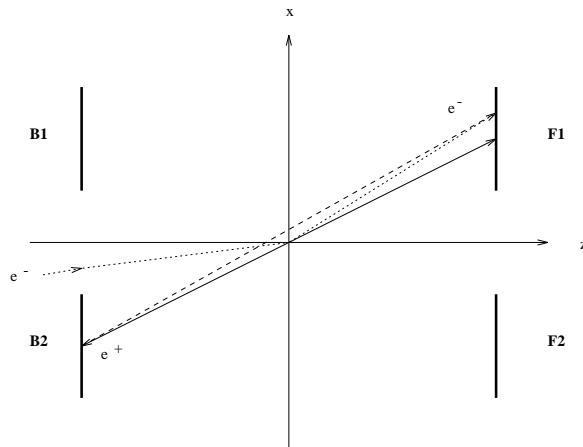
Figure 7: *Effects of the acollinearity and the x displacement on the impact points.*

There are two other useful measures that can be done with the VSAT and which are related to the beam tilt and production angles. With a view to this, it is helpful to consider events with equal (positive) beam tilt angles, θ^x_+ and θ^x_-, as in fig. 8. The
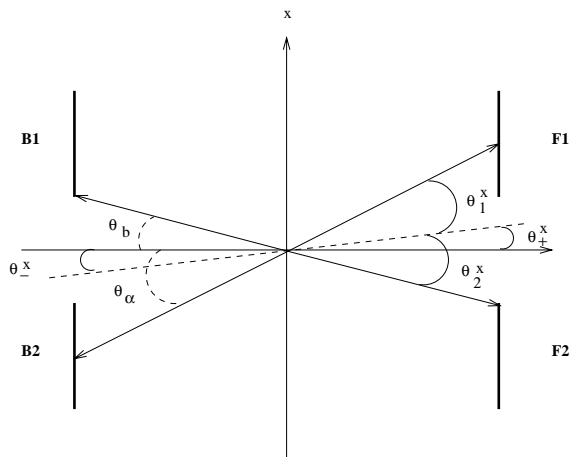
Figure 8: *Effect of the beam tilts on the production angles on the two diagonals.*

figure shows clearly that the (average) production angle on diagonal 1, θ^x_1, is smaller than in the case of zero tilts, where it would be equal to θ_a. The opposite holds for the

production angle on diagonal 2: θ_2^x is larger than θ_b. Due to the rapid decrease of the Bhabha cross section with the angle, this induces an opposite variation of the number of accepted Bhabha events on the two diagonals: the number of events on diagonal 1, N_1, will increase, whereas the number of events on diagonal 2, N_2, will decrease. Therefore, we expect to observe a variation of the variable:

$$A_D = \frac{N_1 - N_2}{N_1 + N_2} \tag{11}$$

called *diagonal asymmetry*. It must be noted, however, that the diagonal asymmetry is only affected by the average tilt angle, θ_x, and not by the separate values of θ_-^x and θ_+^x. By consequence, it cannot be used to extract information on the acollinearity, ϵ_x. The relationship between A_D and θ_x has been determined for the average conditions of 1993 and 1994 data taking [5] by extensive Monte Carlo simulation production using FASTSIM, which is used in order to caclulate the luminosity. The runs had about 4000 Bhabha events each and were done with different x interaction point values, different beam widths, divergences, tilts and acollinearities.

Finally, from eq. (9), we see that the average value $R\Delta x_0$ of the combined widths $R\Delta x_1$ and $R\Delta x_2$ of the Δx_1 and Δx_2 distributions is related to the widths σ_x and σ_z of the incident beams at the interaction point and to their divergences in the (x,z) plane.

2.2   Beam parameters in the (y,z) plane

The situation in this plane is analogous to what we saw in the previous section for the (x,z) plane, the only difference being that the superconducting quadrupoles have a convergent rather than a divergent effect. This induces a focusing of the scattered particle trajectories in the y direction, which in turn causes the detector to loose sensitivity.

We will repeat the calculations of section 2.1 briefly. First, we consider the simple case of no beam displacement and zero tilts (fig. 9). The modules have been moved to
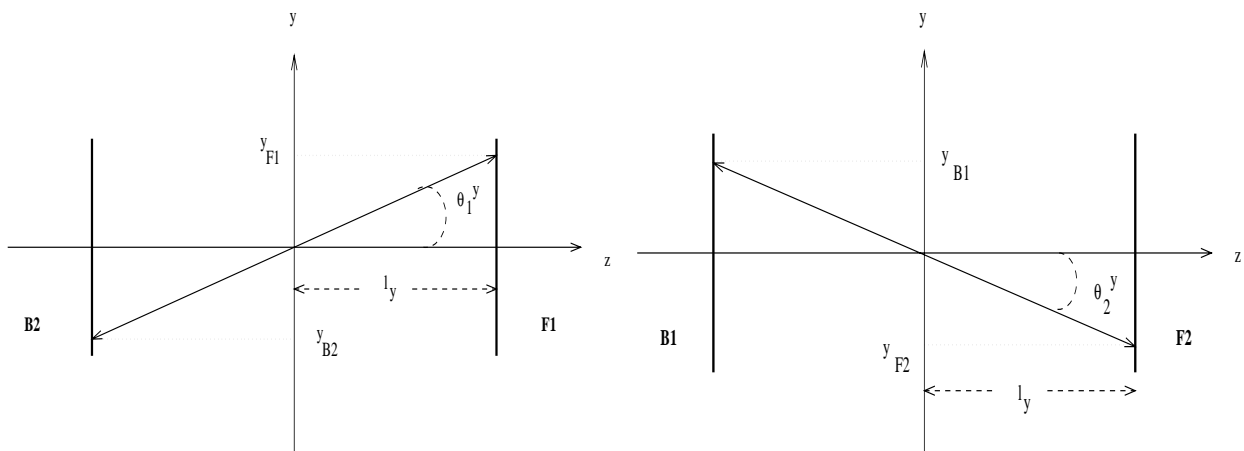
Figure 9: *Events on diagonals 1 and 2 for zero beam displacement and zero tilts.*

an effective distance, $l_y = 3.5$ m, due to the convergent effect of the quadrupoles. The same assumptions as in the case of the (x,z) plane apply here as well, i.e. l_y is the same

for all modules and the production angles on the two diagonals, θ_1^y and θ_2^y, are defined to be positive. The y coordinates of the impact points of the outgoing particles on the four modules are then given by

$$y_{F1} = l_y\theta_1^y \qquad y_{B2} = -l_y\theta_1^y \qquad y_{B1} = l_y\theta_2^y \qquad y_{F2} = -l_y\theta_2^y \tag{12}$$

The next step is to include a beam displacement in y, y_b. The factor f_y is of the order of 0.1. From fig. 10 we can calculate the y coordinates:

$$y_{F1} = f_y y_b + l_y\theta_1^y \qquad y_{B2} = f_y y_b - l_y\theta_1^y$$

$$\tag{13}$$

$$y_{B1} = f_y y_b + l_y\theta_2^y \qquad y_{F2} = f_y y_b - l_y\theta_2^y$$
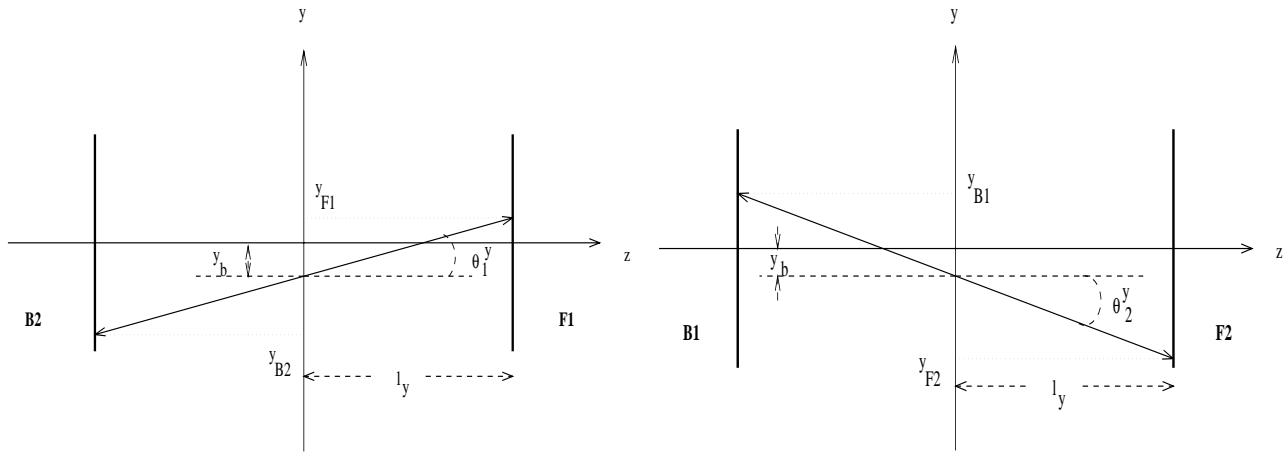
Figure 10: *Events on the two diagonals for zero z displacement and zero tilts.*

We define

$$\Delta y_1 = y_{F1} + y_{B2} \qquad \Delta y_2 = y_{F2} + y_{B1} \tag{14}$$

The effect of a shift of y_b on those variables is similar to that of a shift of x_b on the corresponding quantities of the (x,z) plane: from the last equations we have $\Delta y_1 = \Delta y_2 = 2f_y y_b$, therefore the variables Δy_1, Δy_2 and $\Delta y_0 = (\Delta y_1 + \Delta y_2)/2$ vary proportionally to y_b, whereas the difference $\Delta y_1 - \Delta y_2$ is always zero. We can now continue to consider the situation presented in fig. 11, where we have assumed a positive z displacement, z_b. From the figure, we obtain

$$y_{F1} = f_y(y_b - z_b\theta_1^y) + l_y\theta_1^y \qquad y_{B2} = f_y(y_b - z_b\theta_1^y) - l_y\theta_1^y$$

$$\tag{15}$$

$$y_{B1} = f_y(y_b + z_b\theta_2^y) + l_y\theta_2^y \qquad y_{F2} = f_y(y_b + z_b\theta_2^y) - l_y\theta_2^y$$

Consequently, the corrected factor is the one including the y_b value, which needs to have subtracted from (diagonal 1) or added to (diagonal 2) a quantity proportionally related
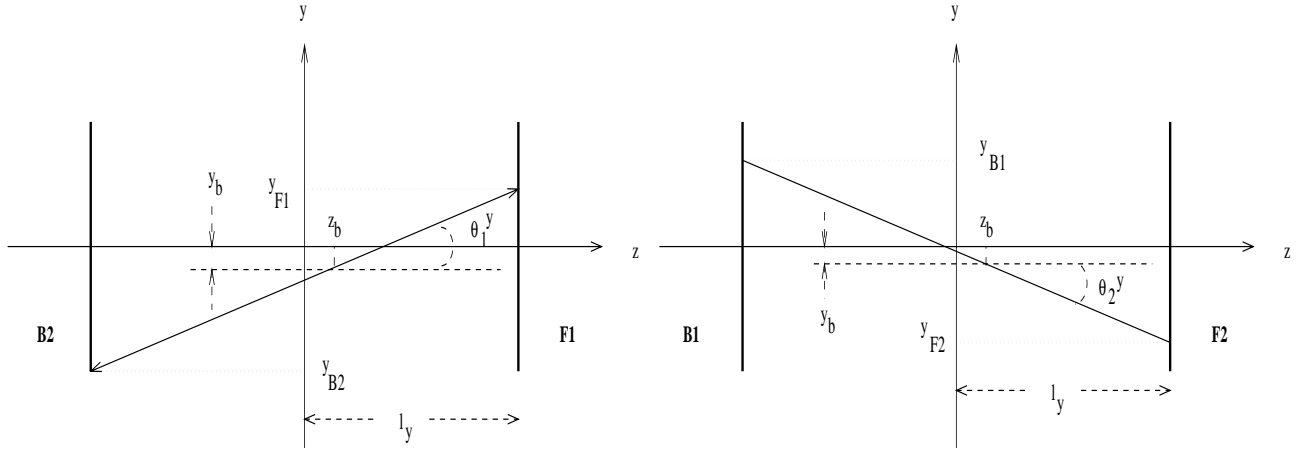
Figure 11: *Events on the two diagonals for nonzero z displacement and zero tilts.*

to z_b. This induces a proportional variation of Δy_1 and Δy_2 with respect to z_b, now being given by

$$\Delta y_1 = 2f_y(y_b - z_b\theta_1^y) \qquad \Delta y_2 = 2f_y(y_b + z_b\theta_2^y) \qquad (16)$$

again including both y_b and z_b in the same equation.

Lastly, the case of nonzero beam tilts has to be mentioned. The y displacement is again taken to be negative while the interaction point is assumed to have no displacement in the z direction. The positron (electron) beam has a positive (negative) tilt denoted by θ_+^y (θ_-^y). The situation is shown in fig. 12, from which it can be derived that
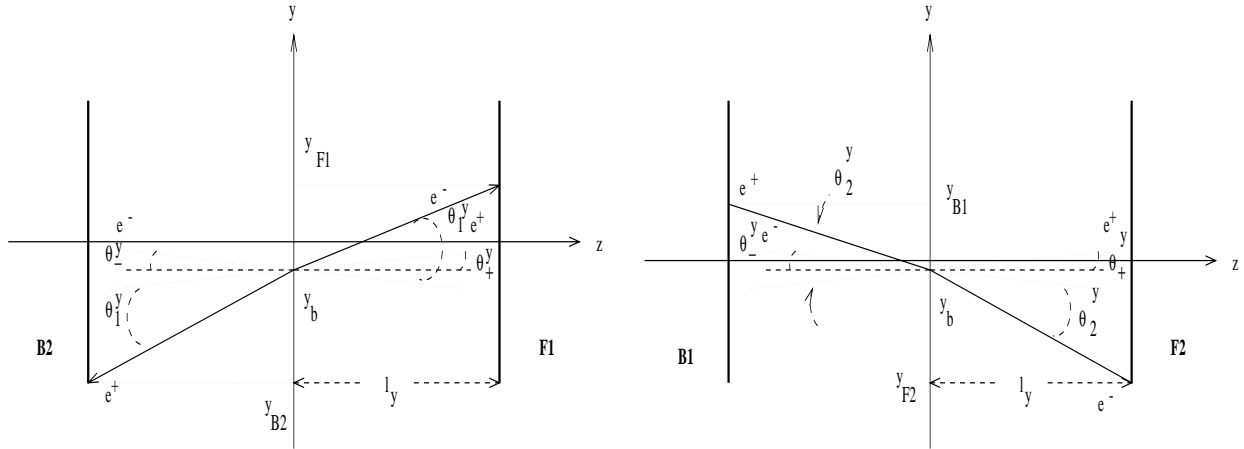
Figure 12: *Events on the two diagonals for zero z displacement and nonzero tilts.*

$$y_{F1} = f_y y_b + l_y(\theta_1^y - |\theta_-^y|) = f_y y_b + l_y(\theta_1^y + \theta_-^y)$$
$$y_{B2} = f_y y_b - l_y(\theta_1^y + |\theta_+^y|) = f_y y_b - l_y(\theta_1^y + \theta_+^y)$$

$$(17)$$

$$y_{B1} = -|f_y y_b| + l_y(\theta_2^y - |\theta_+^y|) = f_y y_b + l_y(\theta_2^y - \theta_+^y)$$
$$y_{F2} = f_y y_b - l_y(\theta_2^y + |\theta_-^y|) = f_y y_b - l_y(\theta_2^y - \theta_-^y)$$

The acollinearity in the (y,z) plane, $\epsilon_y = \theta_-^y - \theta_+^y$, affects the y coordinates of the impact points in the same way as y_b does, as can be seen in the following equation:

$$\Delta y_1 = \Delta y_2 = 2 f_y y_b + l_y(\theta_-^y - \theta_+^y) \tag{18}$$

By combining our conclusions so far, we can derive the equations for the case of both nonzero y and z displacement and nonzero tilts:

$$y_{F1} = f_y(y_b - z_b(\theta_1^y + \theta_-^y)) + l_y(\theta_1^y + \theta_-^y) \qquad y_{B2} = f_y(y_b - z_b(\theta_1^y + \theta_+^y)) - l_y(\theta_1^y + \theta_+^y)$$

$$(19)$$

$$y_{B1} = f_y(y_b + z_b(\theta_2^y - \theta_+^y)) + l_y(\theta_2^y - \theta_+^y) \qquad y_{F2} = f_y(y_b + z_b(\theta_2^y - \theta_-^y)) - l_y(\theta_2^y - \theta_-^y)$$

from which

$$\Delta y_1 = 2 f_y(y_b - z_b(\theta_1^y + \theta_y)) + l_y \epsilon_y \qquad \Delta y_2 = 2 f_y(y_b + z_b(\theta_2^y - \theta_y)) + l_y \epsilon_y \tag{20}$$

Using the average values of Δy_1 and Δy_2 over one cassette we conclude that

$$\Delta y_0 = 2 f_y y_b + l_y \epsilon_y - f_y z_b(\theta_1^y - \theta_2^y + 2\theta_y) \tag{21}$$

The average values of θ_1^y and θ_2^y are very close to zero and also the product $f_y z_b \theta_y$ is extremely small, so the third term in the righthand side of eq. (21) is completely negligible.

One can also define the difference δy:

$$\delta y = \Delta y_2 - \Delta y_1 = 2 \cdot f_y z_b(\theta_1^y + \theta_2^y) \tag{22}$$

but, due to the very small values of f_y, θ_1^y and θ_2^y, δy is practically zero and thus carries no useful information on z_b.

3 Determination of the beam parameters

From VSAT data alone we can estimate the z coordinate of the interaction point using eq. (10), but this is not possible neither for the x nor for the y coordinate. This is due to the fact that, as shown in eq. (9) and (21), the detector variables depend both on the beam displacement and on the acollinearity in those directions. However, we can use the beamspot values for x and y as they are determined by VD and TPC to obtain information on the variations of the acollinearity.

3.1 Estimation of the x beamspot

The evolution of Δx during 1994 data taking is shown in fig. 13 (we recall that Δx represents the average value over the events of a cassette).

Due to the limited VSAT acceptance in the x direction, this average value must be corrected, since Δx_1 and Δx_2 represent average values of rather broad distributions, which
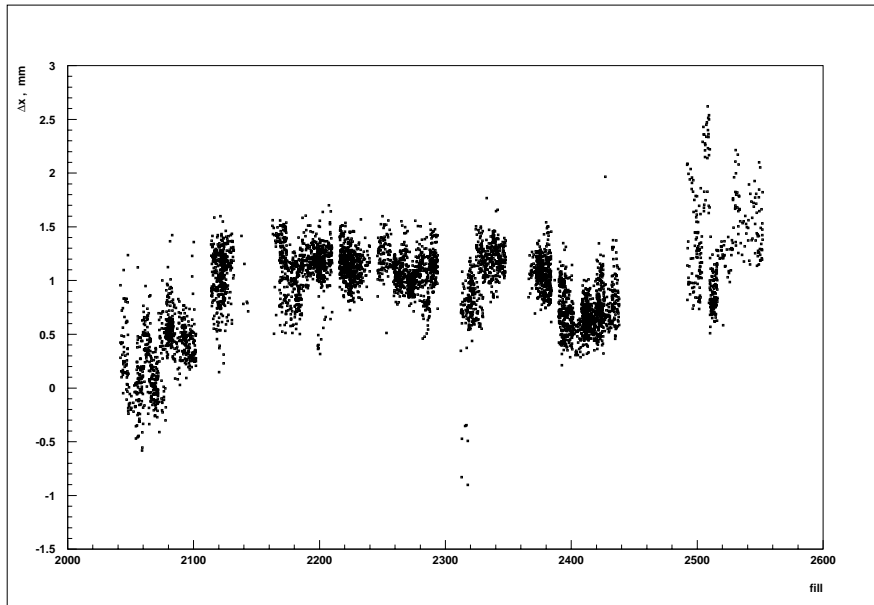
Figure 13: *Variations of Δx during 1994 data taking.*

are affected in non trivial ways by different beam parameters, such as beam width, divergence and acollinearity. Furthermore, the averaging procedure introduces a dependence of Δx_1 and Δx_2 on the y tilt. FASTSIM has shown that these effects can be parametrized in terms of quantities directly measured by the VSAT. The correction for the beam width and divergence effect can be expressed as a dependence on the widths of the Δx_1 and Δx_2 distributions, $R\Delta x_1$ and $R\Delta x_2$, respectively; the correction for the tilt in y can be achieved through the Δy_1 and Δy_1 distributions. The resulting relations are then [6]

$$\Delta x_{1C} = \Delta x_1(1 + 0.1(R\Delta x_1 - 2.6)) - 0.1(\Delta y_1 + 7)$$

$$\Delta x_{2C} = \Delta x_2(1 + 0.1(R\Delta x_2 - 2.8)) - 0.05(\Delta y_2 + 8)$$

(23)

Consequently, Δx_0 and δx of eqs. (9) and (10) should be replaced by the quantities $\Delta x_C = (\Delta x_{1C} + \Delta x_{2C})/2$ and $\delta x_C = \Delta x_{2C} - \Delta x_{1C}$, respectively. It is convenient to define the quantity x_{int} as follows:

$$x_{int} = \frac{\Delta x_C}{2f_x}$$

(24)

It is then clear that, from eqs. (9) and (24),

$$x_{int} = x_b + \epsilon_x \frac{l_x}{2f_x} + x_0$$

(25)

where we have included in the offset x_0 the small term $\frac{z_b}{2}(\theta_2^x - \theta_1^x - 2\theta_x)$ of eq. (9), which is practically constant, since θ_1^x and θ_2^x are practically equal and θ_x is very small.

As evident from eq. (25), x_{int} is more directly related to x_b. The 1994 values of x_{int} and the period limits are shown in fig. 14 (period 1: fills 2042 to 2140, period 2: fills 2167 to 2435, period 3: fills 2493 to 2551). In the first fills, x_{int} had negative values but

close to zero and was increasing during period 1, at the end of which it had reached 300 μm. In period 2, its values decreased by 100 μm approximately, whereas it displayed an increase of about 200 μm between fills 2510 and 2530 of period 3. The intervals covered by x_{int} for the three periods are shown in fig. 15. The corresponding mean values are: 123 μm, 244 μm and 297 μm, whereas that for the year is 223 μm.
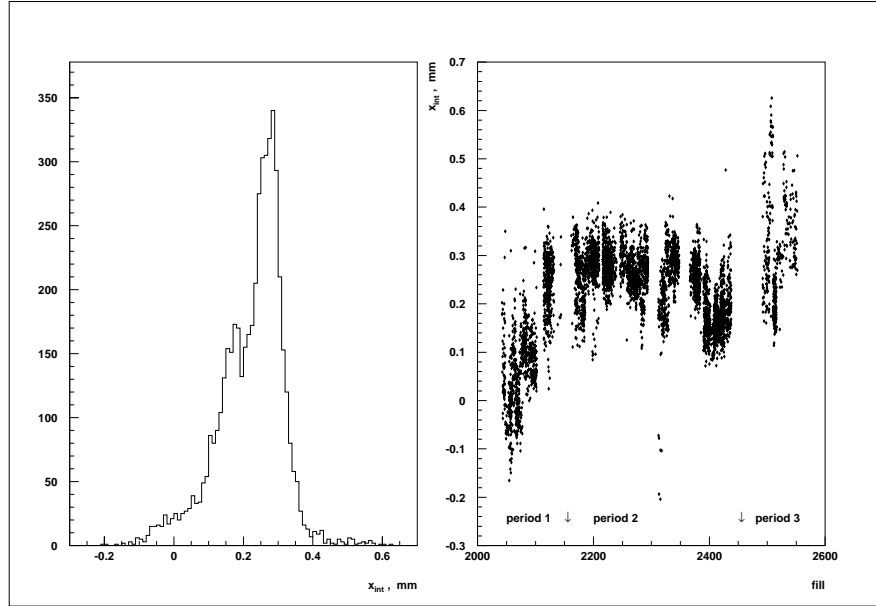
Figure 14: x_{int} from 1994 VSAT data with corrections for the beam width, divergence and y-tilt. The x-acollinearity effect has not been included.
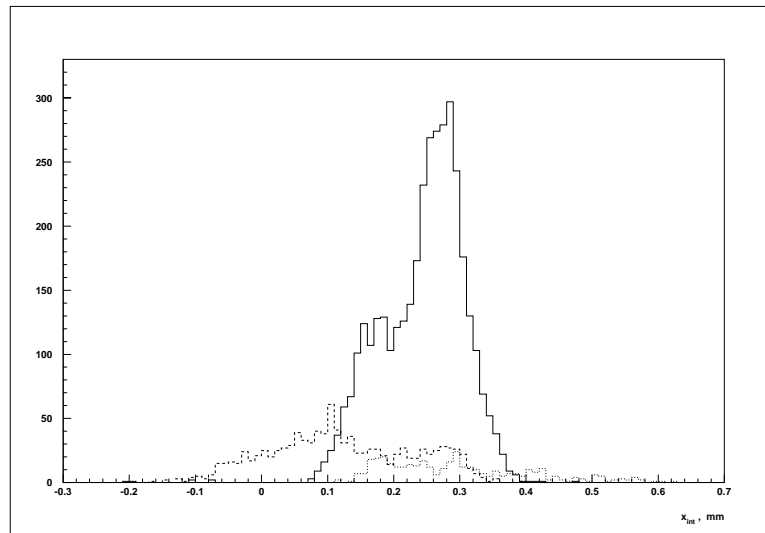
Figure 15: Distributions of x_{int} for periods 1 (dashed line), 2 (full line) and 3 (dotted line), 1994 data.

In fig. 16, we show the estimation of x_{int} for 1993 data and the relevant variation during the year. 1993 data show a more uniform behaviour for periods 1 and 2 (thus treated as one period), during which x_{int} increased by 200 μm (fig. 16). In the third period, x_{int} was rather stable, while the step between period 2 and period 3 is 300 μm. Consequently, there are differences between 1994 and 1993 data both as for the steps between periods and as for the amount of the fluctuation within each period. The trends in 1993 data are more moderate than those of 1994 data. The step in 1993 values is, however, by far more impressive than those observed during 1994, which were 50 μm from period 1 to period 2 and 150 μm from period 2 to period 3. The overall mean value of the 1993 distribution was 110 μm (to be compared with 223 μm for 1994), whereas that of the first two periods was 29 μm (much smaller than any of the mean values of 1994) and that of the third period was 457 μm (larger than the largest mean value of 1994 (period 3) by 160 μm). The transition from period 2 to period 3 in 1993 data is also visible in the distribution of x_{int}, where we see two peaks separated by 450 μm. Such a behaviour has not been observed in 1994 data.
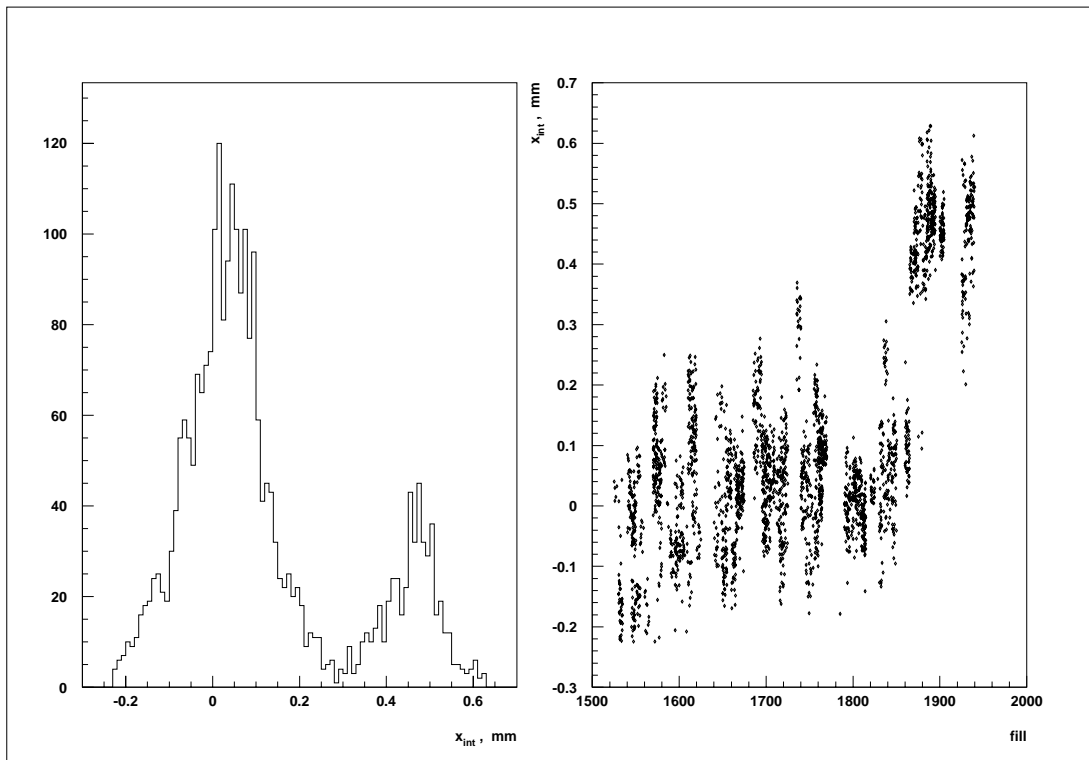
Figure 16: x_{int} *for 1993 data.*

In figs. 17 and 18, we have plotted the x beamspot estimations by the Micro Vertex detector (VD) for 1994 and 1993, respectively. When comparing with VSAT values for x_{int}, we observe the same trends during the periods but in a more moderate way in the VD data for 1994; this indicates that the effect of the ϵ_x term in eq. (25) is large, as will be discussed below.
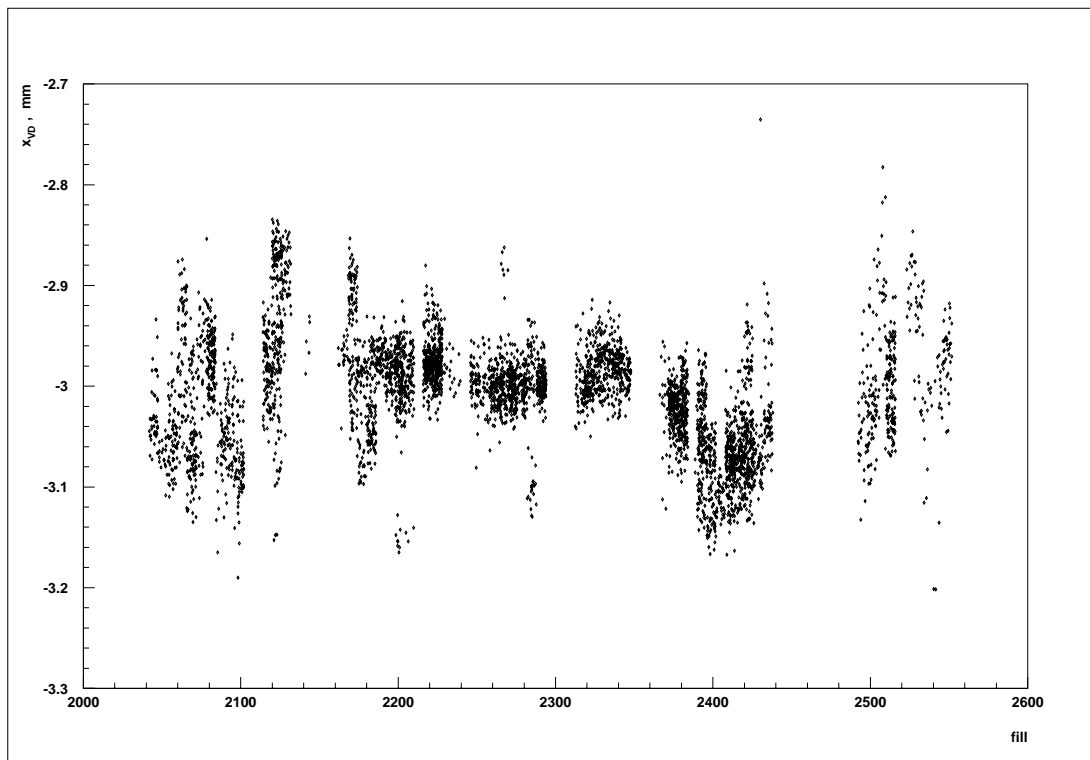
Figure 17: x_{VD} distribution for 1994 data.
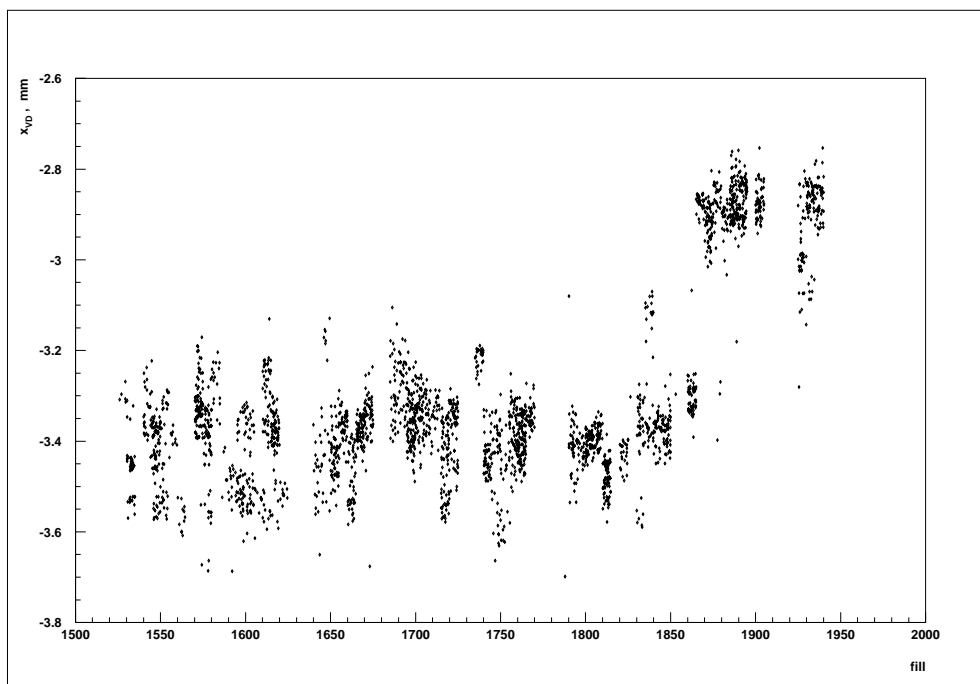
Figure 18: x_{VD} distribution for 1993 data.

In fig. 19, x_{int} is plotted versus the x of the beamspot measured by the Micro Vertex Detector (VD) for 1994 data. The figure shows a qualitative agreement and suggests a linear relation between the two measurements within an overall shift of the order of 3 mm. This is also shown in fig. 20, which presents the profile plot.
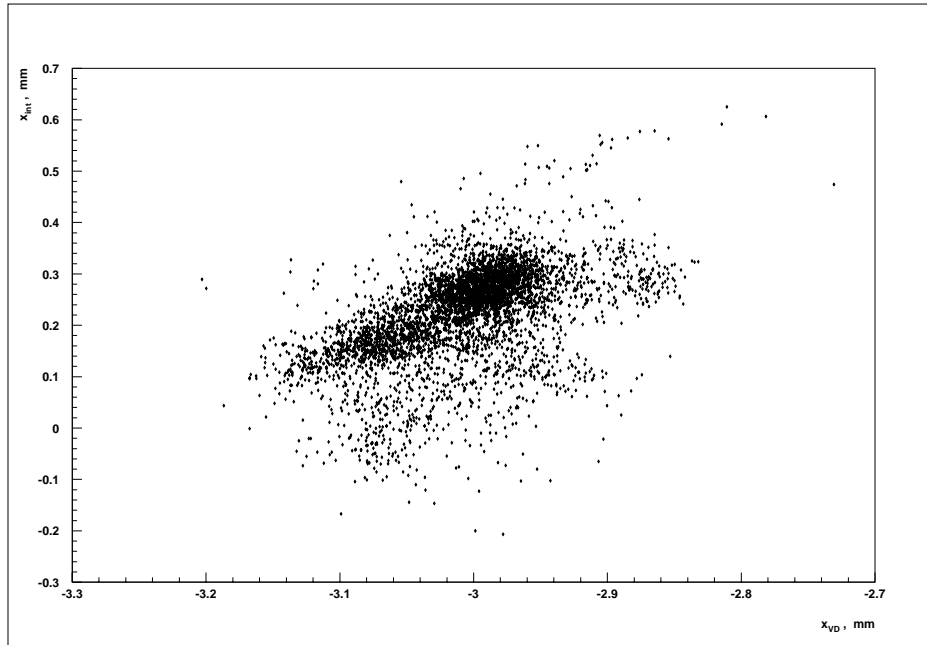
Figure 19: x_{int} from VSAT plotted versus x_{VD} for 1994.
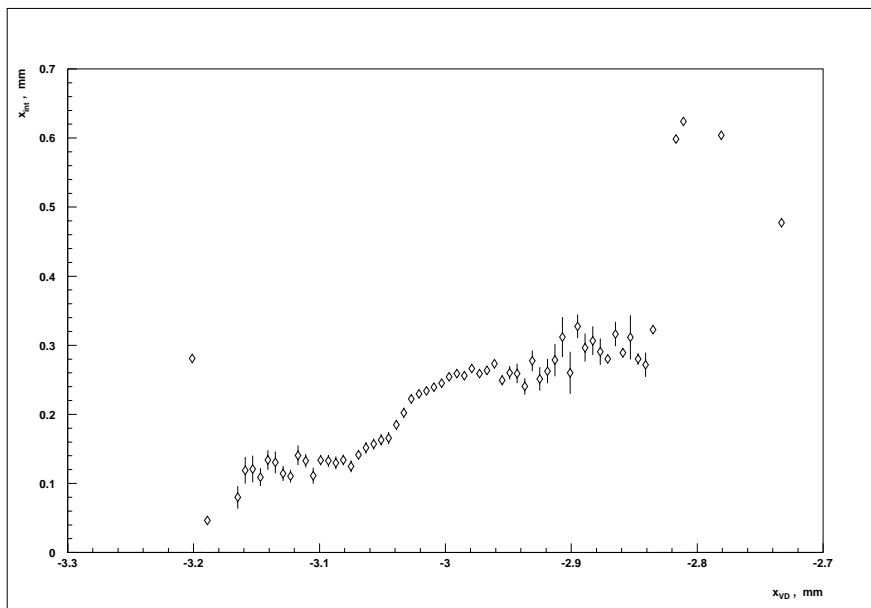
Figure 20: Relation between x_{int} from VSAT and x_{VD} for 1994.

We observe this more clearly in fig. 21, where the distributions of the differences are shown. We observe a shift towards greater values from period 1 to period 2 and a relative increase of the mean value of the gaussian fit by 135 μm. The spread is less in period 2, of the order of 300 μm, smaller than the spread of period 1 by 300 μm. A gaussian fit to the distribution for period 3 would not describe the data. The spread for all periods is significantly larger than the estimated errors (of the order of 18 μm for x_{int} and 12 μm for x_{VD}). The error for the x_{int} measurement is derived from eq. (24) by error propagation. Whenever we make a comparison with VD data, we use average values, x_{int} and x_{VD}, over the same time intervals, i.e. we first find the set of common cassette numbers for the two detectors (as given in the database). The same procedure will be applied later for TPC data.
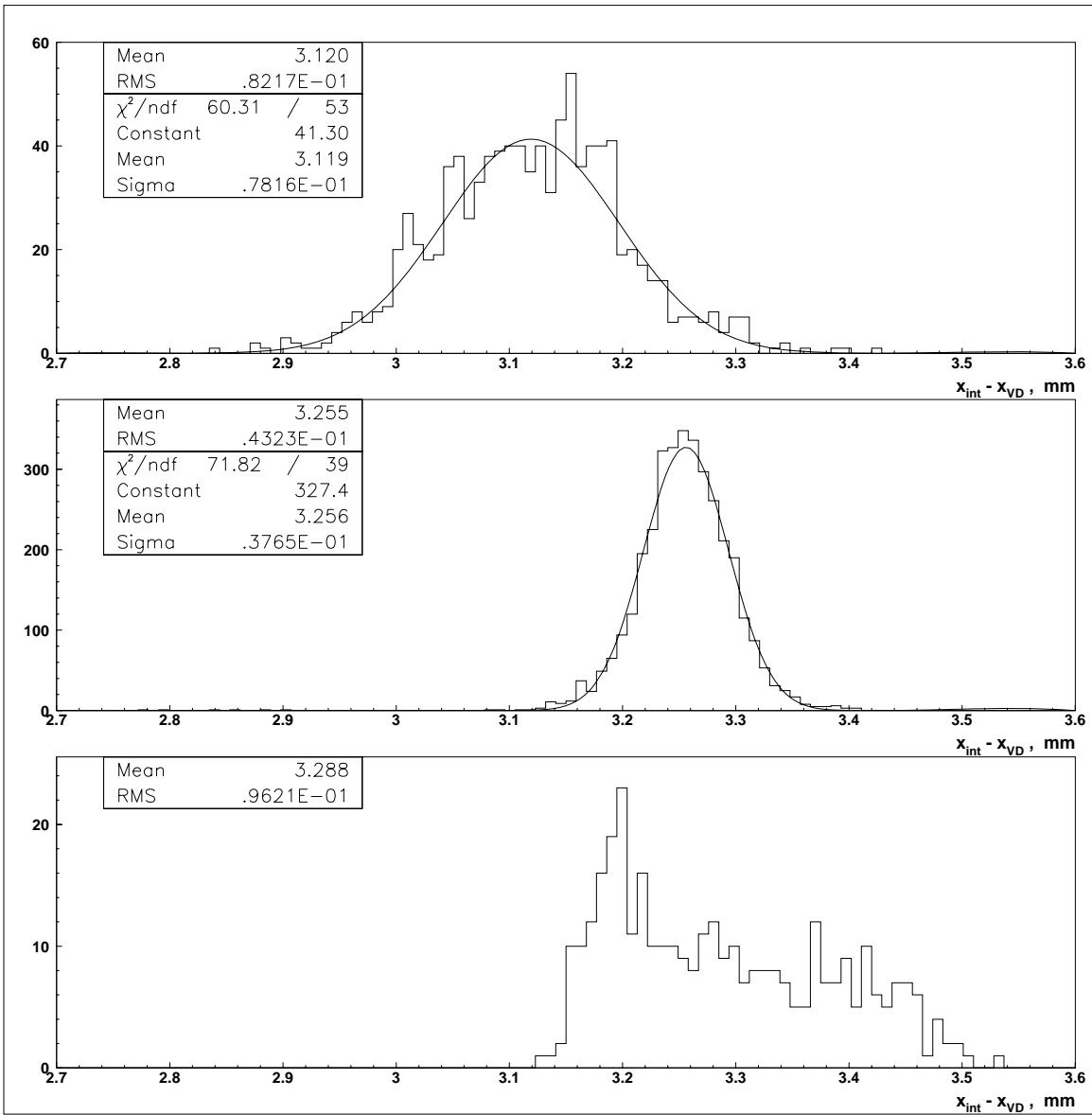
Figure 21: *Difference between x_{int} from VSAT and x_{VD} for the three periods of 1994.*

The spread of the difference distributions can be also seen in fig. 22, where we have plotted the normalized difference to the expected errors in x_{int} and x_{VD} measurements. This difference is given by the relation

$$\delta x_{norm} = \frac{x_{int}- < x_{int} > -(x_{VD}- < x_{VD} >)}{\sqrt{\sigma^2_{x_{int}} + \sigma^2_{x_{VD}}}} \qquad (26)$$

We see that the average fluctuation is about four times the expected value.

Since the VSAT estimation of x_{int} has been done under the assumption of fixed acollinearity, we conclude that the variations of this parameter have a significant contribution to the determination of the interaction point. From FASTSIM simulations done for different beam tilts, we estimate that an average fluctuation in acollinearity of the order of 15 μrad is sufficient to produce an additional variation of about 40 μm in the VSAT determination of x_{int} [3]. This could allow us to assume a systematic difference in acollinearity of about 50 μrad in order to explain the shift of the mean value between period 1 and period 2 (fig. 21).
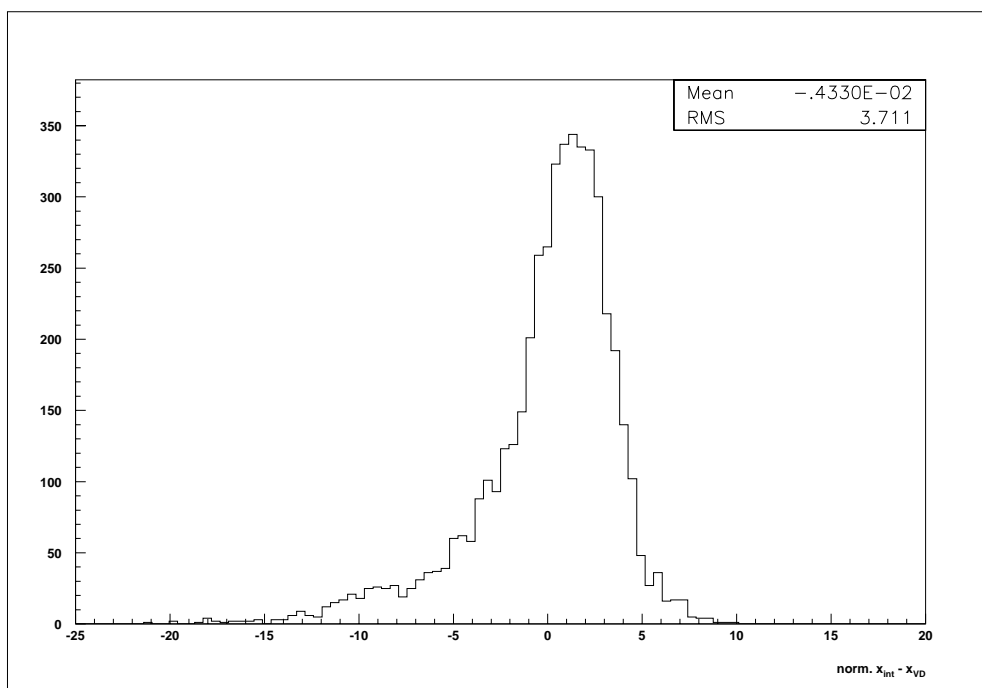
Figure 22: *Normalized difference between x_{int} from VSAT and x_{VD}, 1994 data.*

3.2   Estimation of the y beamspot

As was mentioned in section 2.2, the situation in the (y,z) plane is similar to that in the (x,z) plane, apart from the fact that the effect of the superconducting quadrupoles is here convergent. Eq. (21) is the equivalent of eq. (9) in this plane and we can use it to extract an approximate expression for the y position of the interaction point. In order to achieve

this, we neglect the acollinearity and we obtain the following relation:

$$y_{int} = \frac{\Delta y_1 + \Delta y_2}{4 f_y} \tag{27}$$

The y_{int} distribution is shown in fig. 23, where we have also plotted the variation of this variable during 1994. From the first plot, we see that the majority of the events have been accumulated into two y_{int} intervals. The first peak of low y_{int} values is entirely due to the second period, whereas the main contribution to the second peak comes from period 1. The data from period 3 are also gathered in the high y_{int} interval. The mean values for the three periods are -3.261 cm, -3.936 cm and -3.368 cm, giving an overall mean value of -3.755 cm. The shifts between the three periods are more clearly shown in the second plot of fig. 23, where we observe a step of about 7 mm between period 1 and period 2 and a step of the same order (6 mm) from period 2 to period 3. We also see a decrease of the order of 1 mm within periods 1 and 2 and an increase by the same amount during period 3.
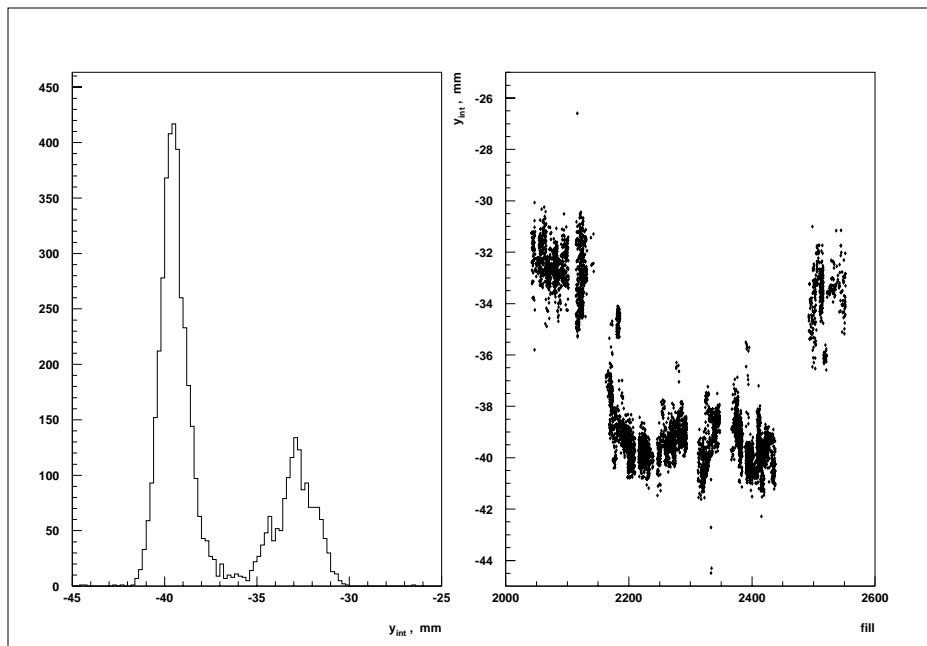
Figure 23: y_{int} from 1994 VSAT data, ϵ_y neglected.

In fig. 24 we have plotted the y_{int} distribution and variation during 1993 data taking. By comparing with fig. 23, we observe that the intervals covered by the data of the two years do not overlap; the 1993 values had been significantly higher, as we also see from the overall mean value for that year: -0.3818 cm, i.e. about a tenth of the corresponding value for 1994. Moreover, the 1993 distribution is more uniform, not including well separated peaks as seen in 1994. The step between 1993 periods 2 and 3 is 2 mm (increase), i.e. about three times smaller than the steps in 1994 data. The variation during period 1-2 was not significant for 1993, whilst there is a decrease of 2 mm during period 3. The 1993 mean values for periods 1-2 and 3 are almost equal (-0.3900 cm and -0.3818 cm, respectively).

The y_{int} VSAT values are plotted versus the y beamspot measurement from VD, y_{VD}, in fig. 25. There is no correlation between the two variables, except within the same period, as shown in fig. 26. This indicates that an acollinearity in the (y,z) plane has to be taken into account, whose effect is probably more significant than the one in the (x,z) plane because of larger variability of y tilts during 1994.
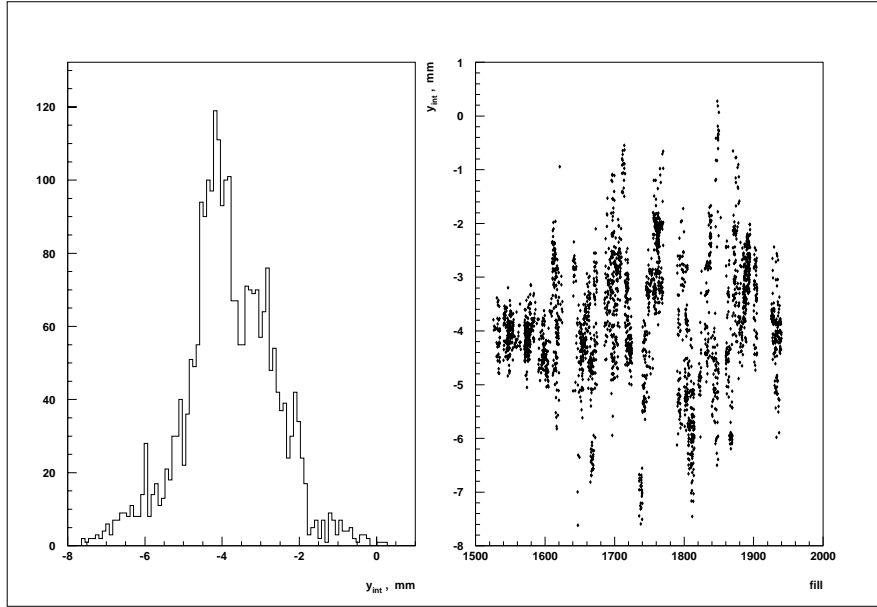
Figure 24: y_{int} from 1993 data, ϵ_y neglected.
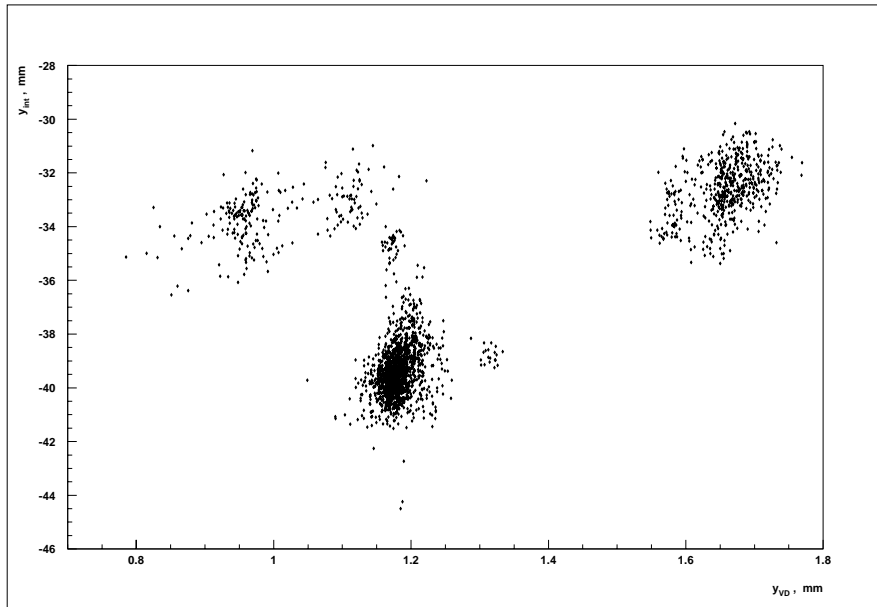
Figure 25: y_{int} from VSAT versus y_{VD}, 1994 data.
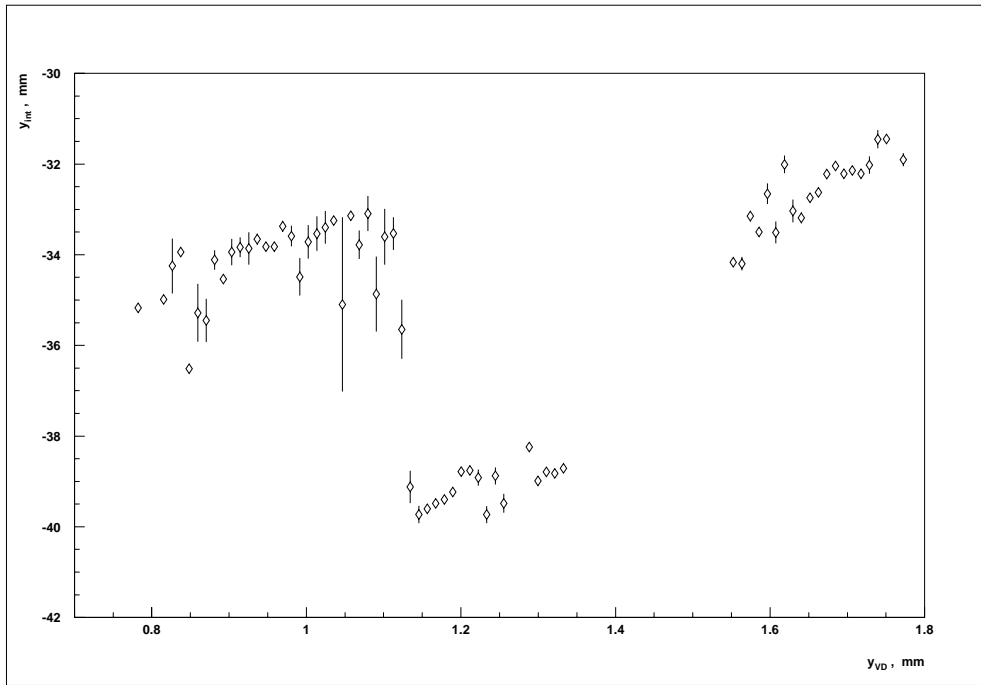
Figure 26: y_{int} from VSAT versus y_{VD}, 1994 data.

As we see in fig. 27, the VD has measured steps between periods 1-2 and 2-3 which were of the order of 500 μm and 200 μm respectively. Tilt angles of about -0.5 mrad are required in order to explain the steps seen between periods in 1994. The lack of
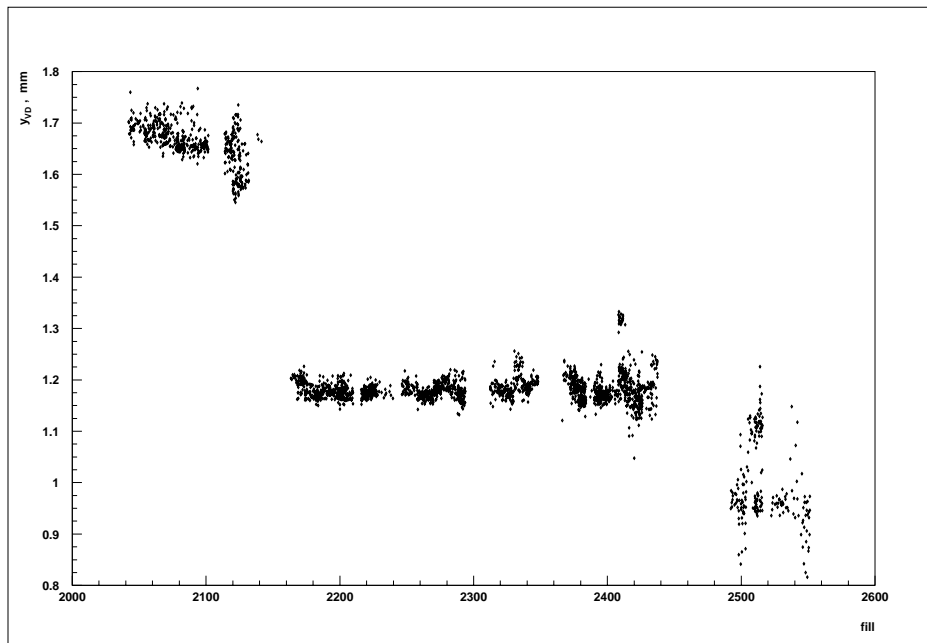
Figure 27: y_{VD}, 1994 data.

correlation between the VSAT and VD measurements of the y interaction point is also present in 1993, as we see by comparing figs. 24 and 28. The VSAT data imply that there are very large tilts in y, which produces the large apparent shifts in y_{int} seen in this analysis.
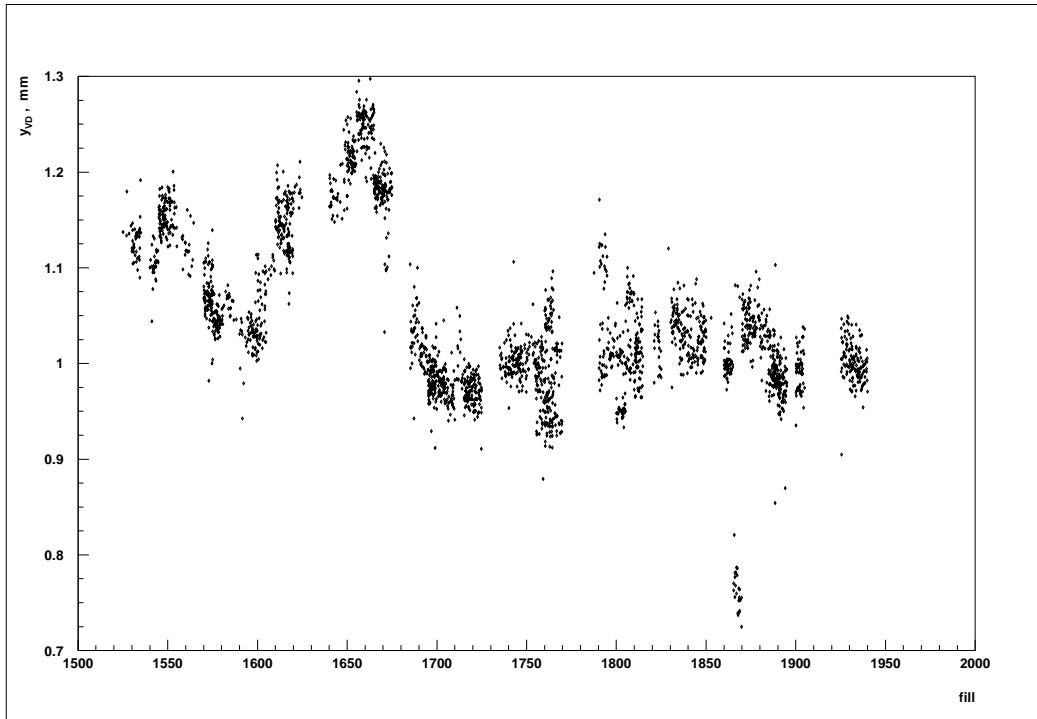
Figure 28: y_{VD}, *1993 data.*

3.3 Estimation of the z beamspot

According to the corrections of section 3.1, from eq. (10), we have

$$z_b = \frac{\delta x_C}{2 f_x (\theta_1^x + \theta_2^x)} \tag{28}$$

The sum of the production angles can be derived from the expressions of the impact points, eq. (6), as follows:

$$\theta_1^x + \theta_2^x = \frac{x_{F1} - x_{B2} - x_{F2} + x_{B1}}{2 \cdot l_x} \tag{29}$$

The distribution of z_b during 1994 is given in fig. 29. We observe an increase by 5 mm during period 1; the values in period 2 increased by 1 mm from fill 2250 to fill 2350 and decreased by a few mm during the rest of the period. There are no steps between periods in fig. 29. The only shifts we can see are in the mean values, which are -26.21 mm for the first period, -26.85 mm for the second period and -29.10 mm for the third period. The mean for the overall distribution is -26.89 mm. On the whole, z_b had been varying over the same interval in all periods.
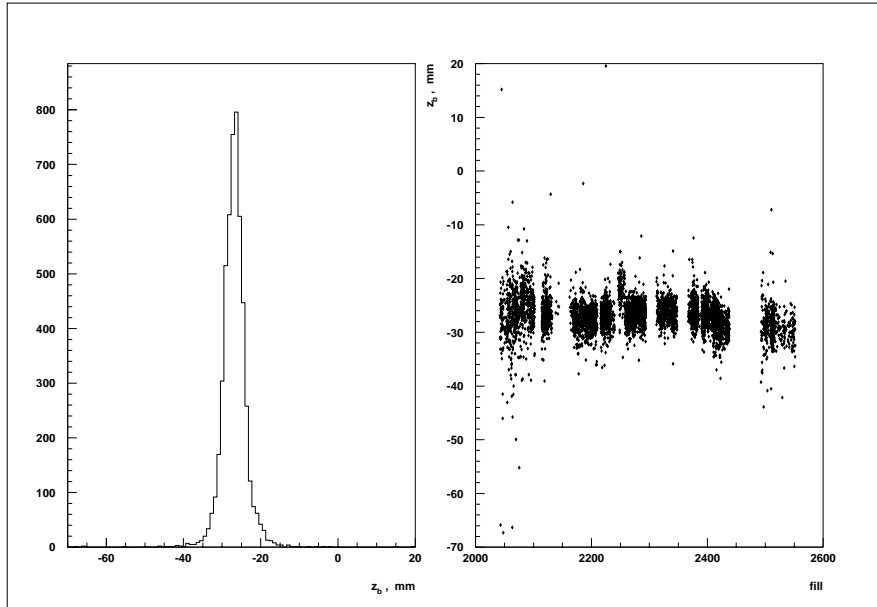
Figure 29: *z beamspot from Δx_1 and Δx_2, 1994 data.*

In fig. 30, we have plotted the distribution and variation of z_b during 1993 data taking. By comparing with fig. 29, we observe almost the same spread around the mean values for the two years (of 1.5 cm for 1994 and 1 cm for 1993) but the 1993 distribution was almost symmetric around zero, i.e. there is a shift in mean values from 1993 to 1994 of the order of -3 cm.
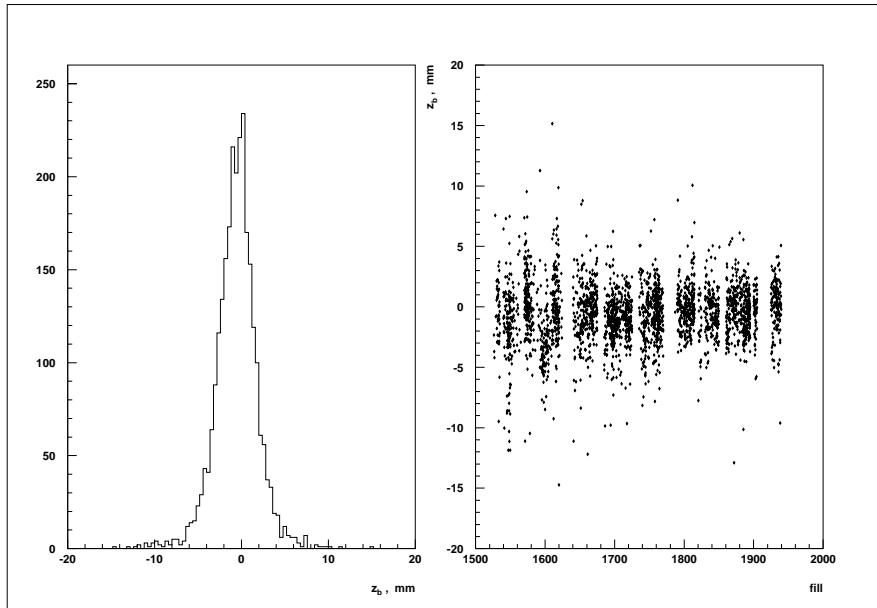
Figure 30: *z_b from 1993 data.*

As for the trends within individual periods, 1993 had been more moderate than 1994: z_b had increased from -1 mm to 0 mm by the end of the second period and then varied from negative to positive values (each case covering about half of the period), increasing by 1.5 mm. In 1994 data, we had mostly negative values. The steps between 1993 periods are negligible, as was the case for 1994, while the mean values for periods 1-2 and period 3 were -0.6625 mm and -0.2028 mm, respectively; the mean value for the year was -0.5743 mm.

In fig. 31, we have plotted the VSAT versus the TPC measurement for the z beamspot. We discern a linear relation as in the case of x_{int} (fig. 20) but with a reduced spread of entries around the direction of the fit (fig. 32). The offset between the two measurements is of the order of 20 mm and increases slightly as a function of period, as shown in fig. 34.
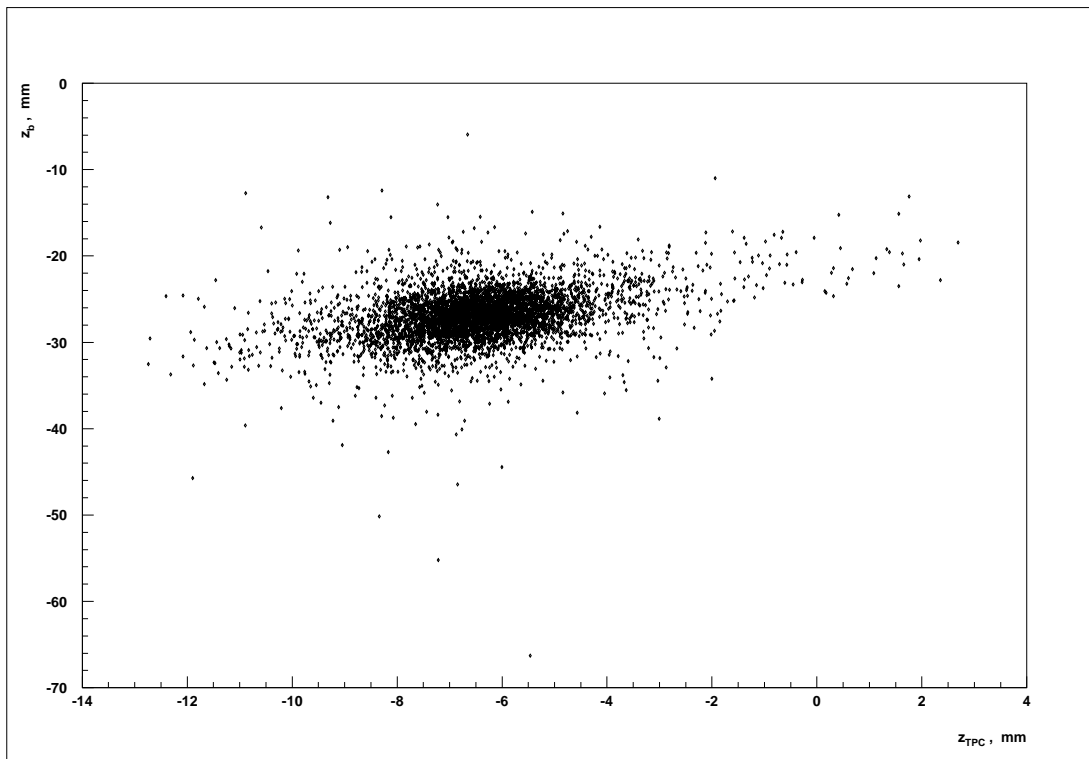
Figure 31: z_b *from VSAT versus* z_{TPC}, *1994 data.*

By comparing figs. 32 and 33, we see that the correlation between the VSAT and TPC measurements of z beamspot was similar in 1993. The offset for that year was of the order of 5 mm (fig. 35), the difference from the 1994 corresponding value being attributed to the 3 cm shift in the z_b values.
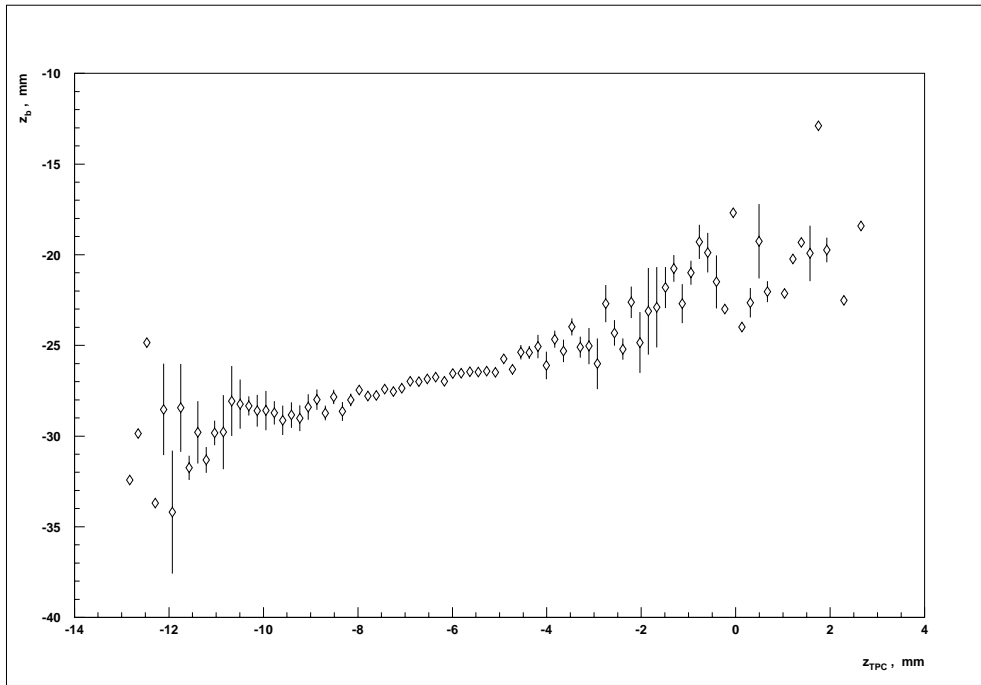
Figure 32: *Correlation between z_b and z_{TPC}, 1994 data.*
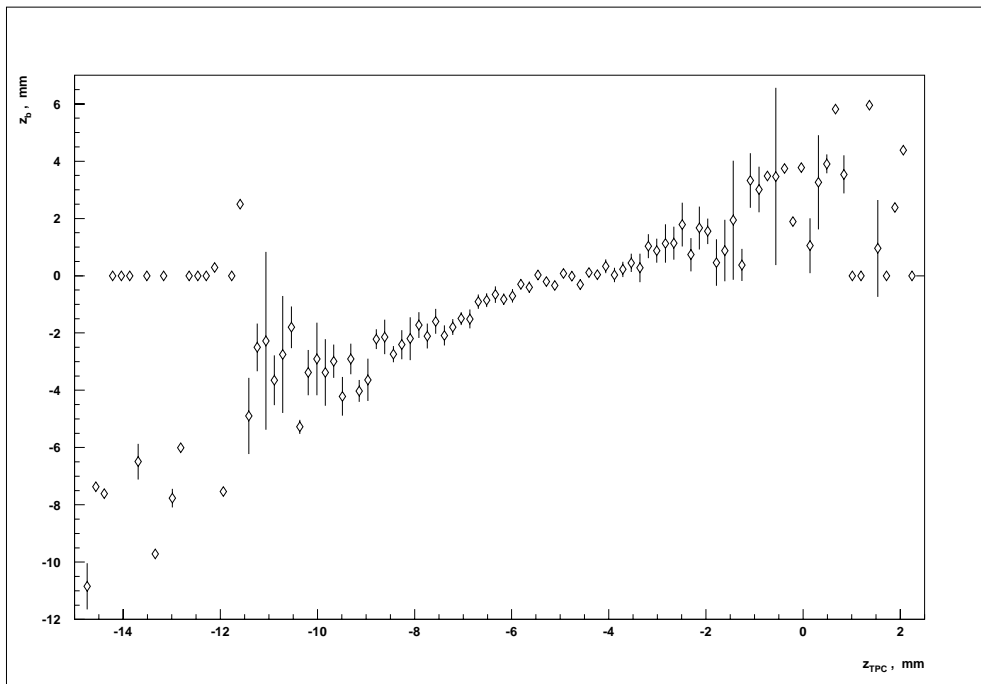
Figure 33: *Correlation between z_b and z_{TPC}, 1993 data.*
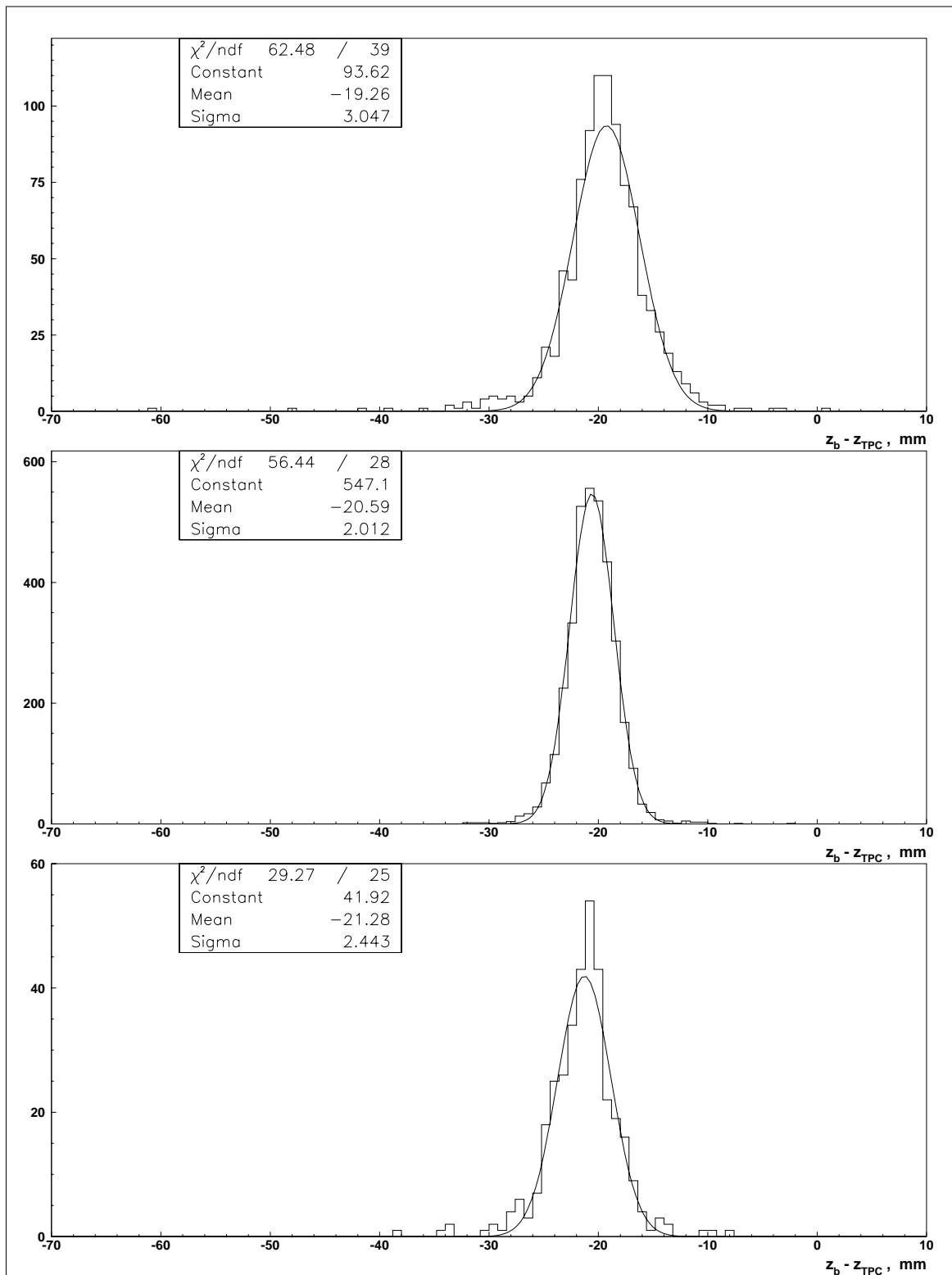
Figure 34: *Difference between z_b and z_{TPC} for the three periods, 1994 data.*

The normalized difference distributions for all 1994 data and for the three periods are given in fig. 36 and 37, respectively.
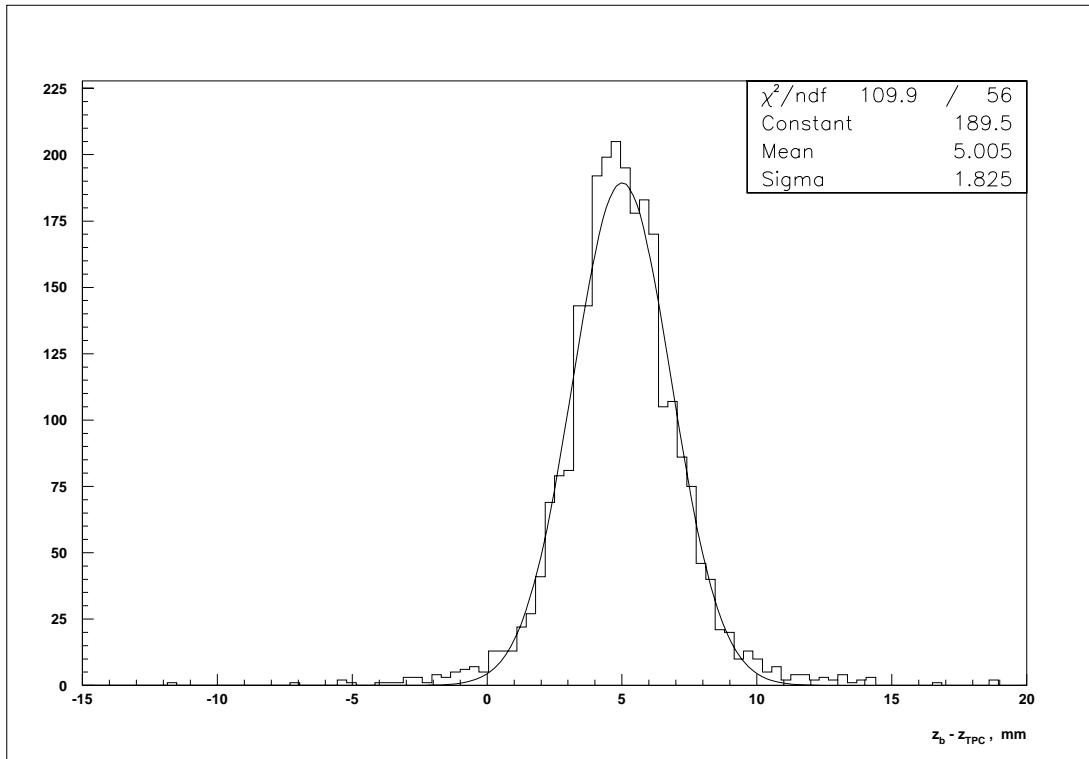
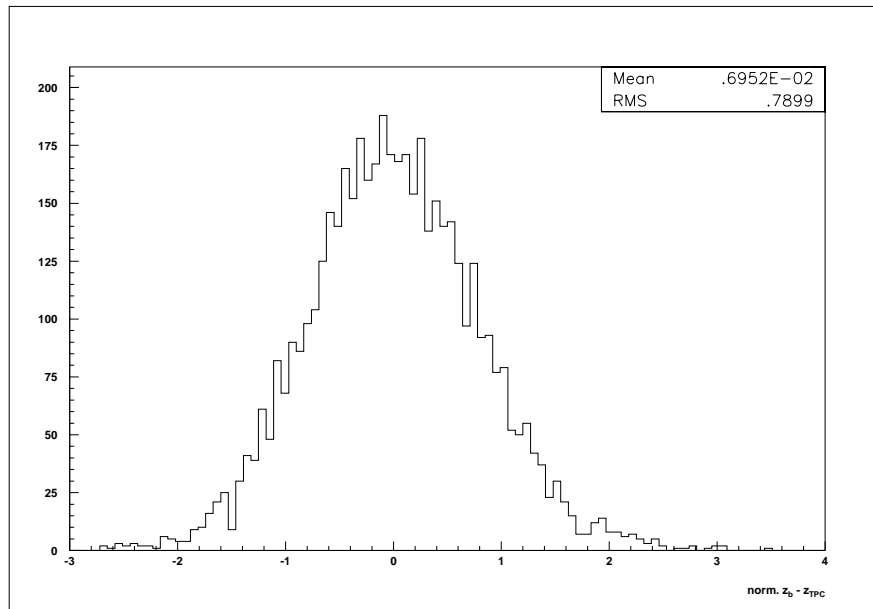Figure 35: *Difference between z_b and z_{TPC}, 1993 data.*

Figure 36: *Normalized difference between z_b and z_{TPC} for all 1994 data.*

As seen by comparing figs. 36 and 22, the correlation between z_b and z_{TPC} is better than the one between x_{int} and x_{VD}. This is due to the fact that the effect of $R\Delta x$ and of
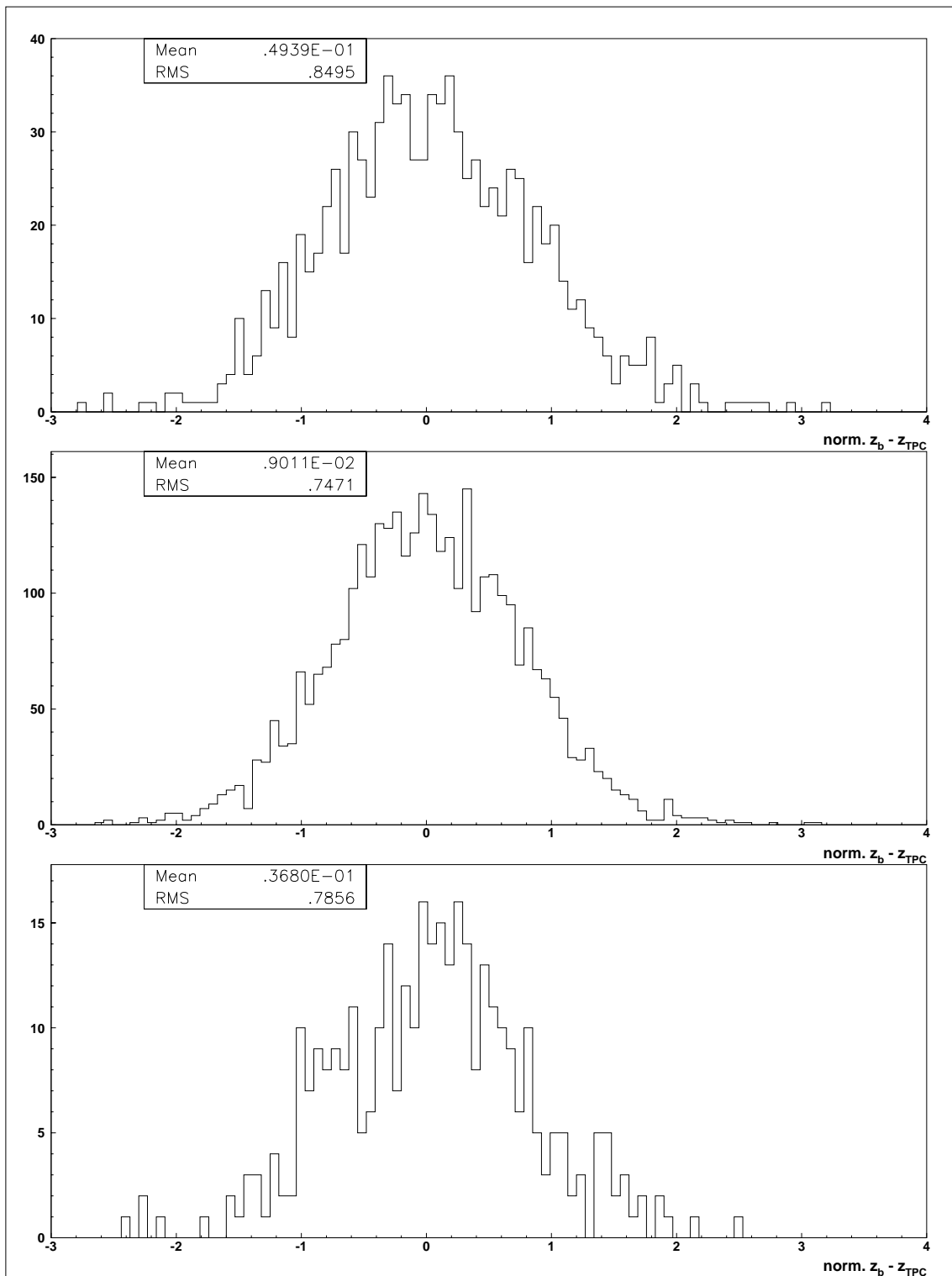
Figure 37: *Normalized difference between z_b and z_{TPC}, 1994 data, periods 1, 2 and 3.*

the acollinearity is smaller on the relation z_b vs $\Delta x_2 - \Delta x_1$ than on the relation between x_{int} and Δx (the dependences cancelling out in the difference). This is also the reason why

we were able to preserve the simplicity of eq. (28) since corrections for the acollinearity, divergences and widths were not necessary in this case.

4 Variation of the asymmetry, acollinearity and tilt.

We can calculate the asymmetry directly from the data by using eq. (11), where N_1 and N_2 are the Bhabha events on diagonals 1 and 2, respectively. As was mentioned in section 2.1, FASTSIM has provided us with a relation between the asymmetry and the mean tilt angle in the (x,z) plane, which allows us to monitor variations of θ_x according to

$$\theta_x = 1.75 \cdot A_D \tag{30}$$

It is possible to estimate the mean tilt, θ_y, in the (y,z) plane from the relations giving the y coordinates of the impact points (eq. (19)):

$$y_{F1} + y_{F2} - y_{B1} - y_{B2} =$$

$$= 2 f_y z_b (\theta_+^y - \theta_-^y) + 2 l_y (\theta_1^y - \theta_2^y + \theta_-^y + \theta_+^y) =$$

$$= -2 f_y z_b \epsilon_y + 2 l_y (\theta_1^y - \theta_2^y) + 4 l_y \theta_y \approx$$

$$\approx 4 l_y \theta_y$$

and thus

$$\theta_y \approx (y_{F1} + y_{F2} - y_{B1} - y_{B2})/4l_y \tag{31}$$

As was mentioned in the previous section, the VD beamspot data can be used to provide us with information on the acollinearity in (x,z) and (y,z) plane. To this end, we introduce the VD values for x beamspot and y beamspot in eqs. (9) and (21), from which we obtain the following expressions:

$$\epsilon_x \approx \frac{\Delta x_C - 2 f_x \cdot x_{VD}}{l_x} \tag{32}$$

and

$$\epsilon_y \approx \frac{\Delta y - 2 f_y \cdot y_{VD}}{l_y} \tag{33}$$

In the following, we present the variations of the beam parameters during 1994 data taking and comment briefly on the their variation during 1993. As was mentioned in section 3.1, the discrepancy between VSAT and VD measurements for the x interaction point can be attributed to the effect of the acollinearity on the VSAT estimation. We expect this influence to be manifest in the variation of x_{int} as well. We can estimate possible additional shifts (due to the acollinearity) by looking into the difference x_{int}-x_{VD} for periods 1, 2 and 3. There is an increase of 150 μm during the first period, which, if indeed due to the acollinearity, suggests a real increase of x_{int} of the order of 300 μm - 150 μm = 150 μm for the first period. In periods 2 and 3, we do not see an acollinearity effect. Since 15 μrad of acollinearity induce a shift of 40 μm in x_{int}, we expect to observe an increase in acollinearity of about 56 μrad for the first period. In fact, fig. 38 shows an increase of the order of 50 μrad for period 1, which agrees with the expected value.

The intervals covered by this parameter during the three periods are from 0.950 mrad to 1.150 mrad in period 1, from 1.025 mrad to 1.150 mrad in period 2 and from 1.040 mrad to 1.180 mrad in period 3. In fig. 39, we see the variation of this parameter during 1993. We observe that 1993 and 1994 have manifested the same general trends as far as 1994 periods 1 and 2 are concerned. The 1993 values of these periods were higher than those of 1994 by 90 μrad for period 1 and by 55 μrad for period 2. In 1994, the mean ϵ_x value increased by 10 μrad from period 2 to period 3 whereas in 1993, it decreased by 45 μrad during the same transition. Both 1994 and 1993 values of the third period were about 1.100 mrad.
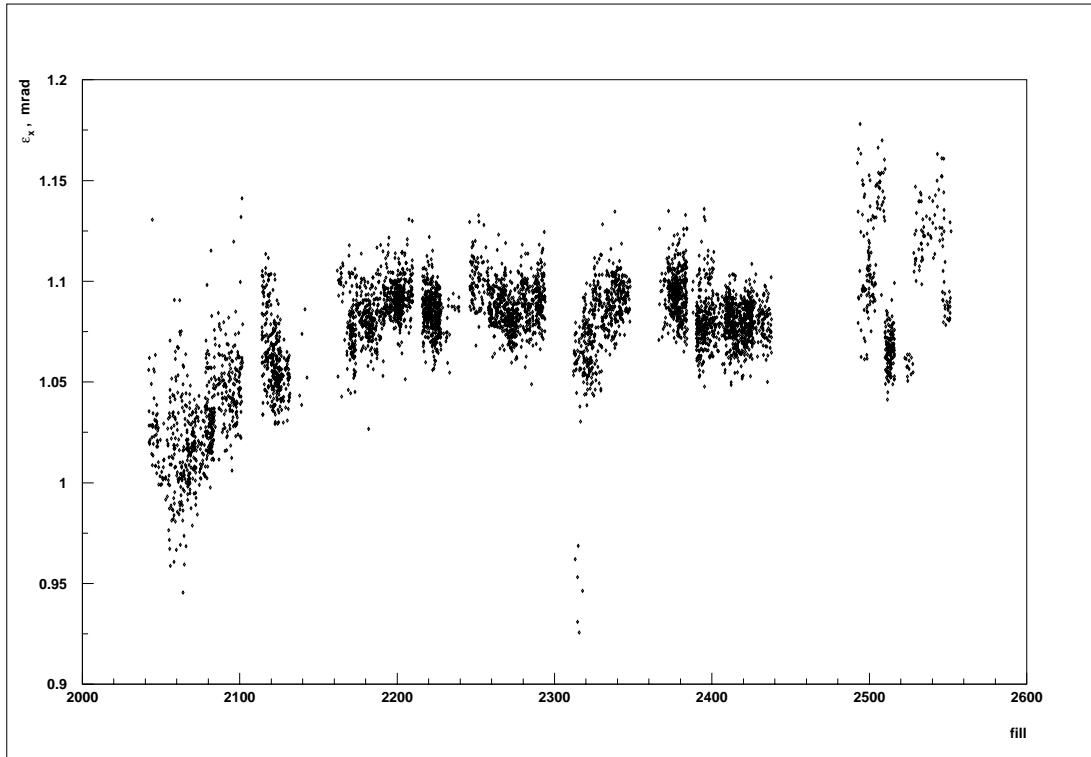
Figure 38: *Variation of ϵ_x during 1994.*
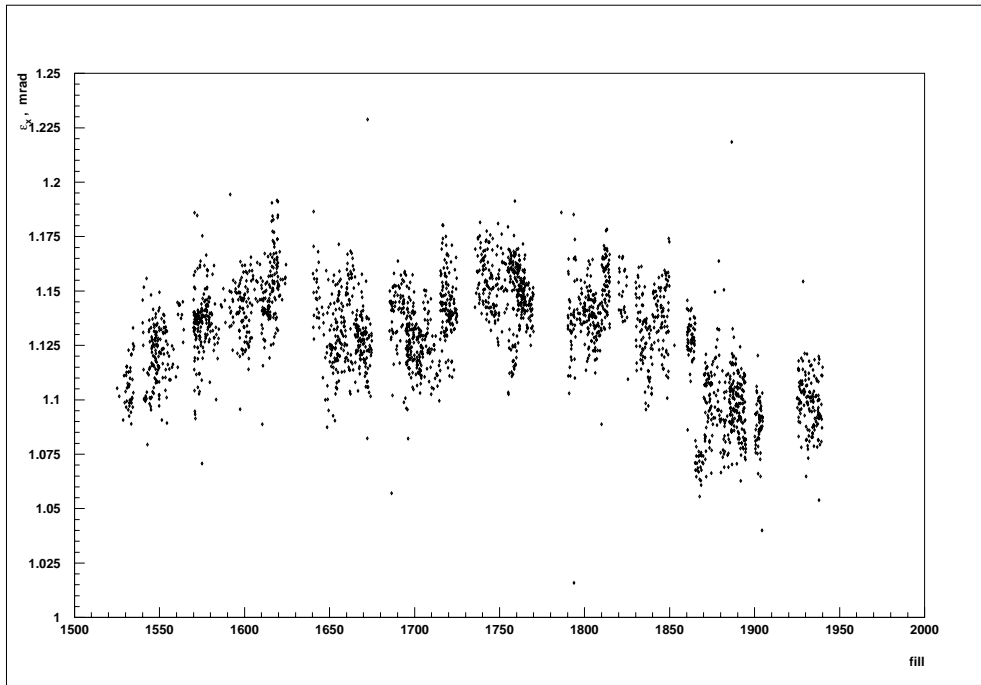
Figure 39: *Variation of ϵ_x during 1993.*

On the other hand, the effect of the beam widths and divergences on the x_{int} values is detected in terms of $R\Delta x$. We show the variations of this parameter for 1994 in fig. 40.
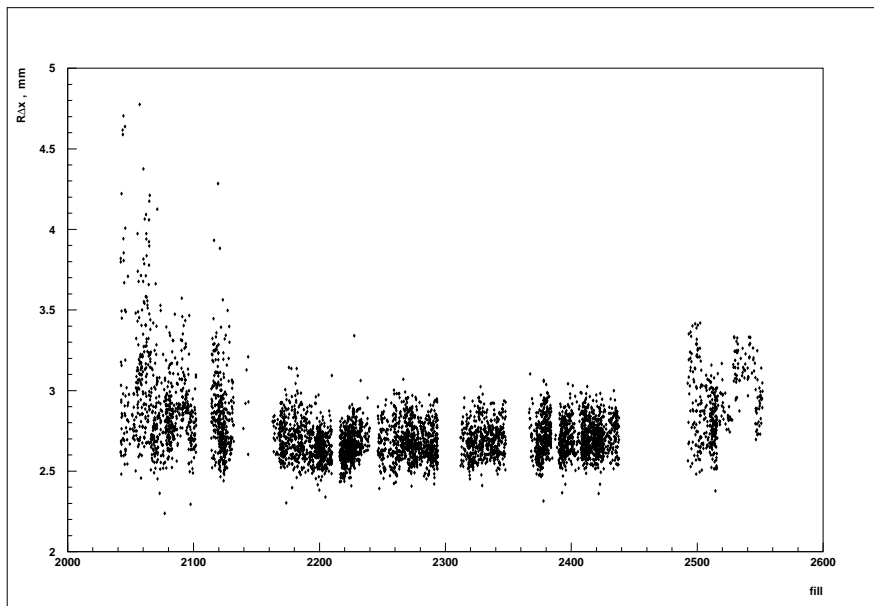
Figure 40: *Variation of $R\Delta x$ during 1994.*

We see that $R\Delta x$ varied from 2.2 mm to 4.8 mm in period 1, from 2.2 mm to 3.4 mm in period 2 and from 2.2 mm to 3.5 mm in period 3. There is an increase of the order of 50 μm during period 2. In fig. 41, the variation of $R\Delta x$ during 1993 is plotted. We see that this variable covered a smaller interval in 1993 than in 1994, i.e. from 2.4 mm to 3.4 mm, within which it manifested more moderate fluctuation than in the following year.
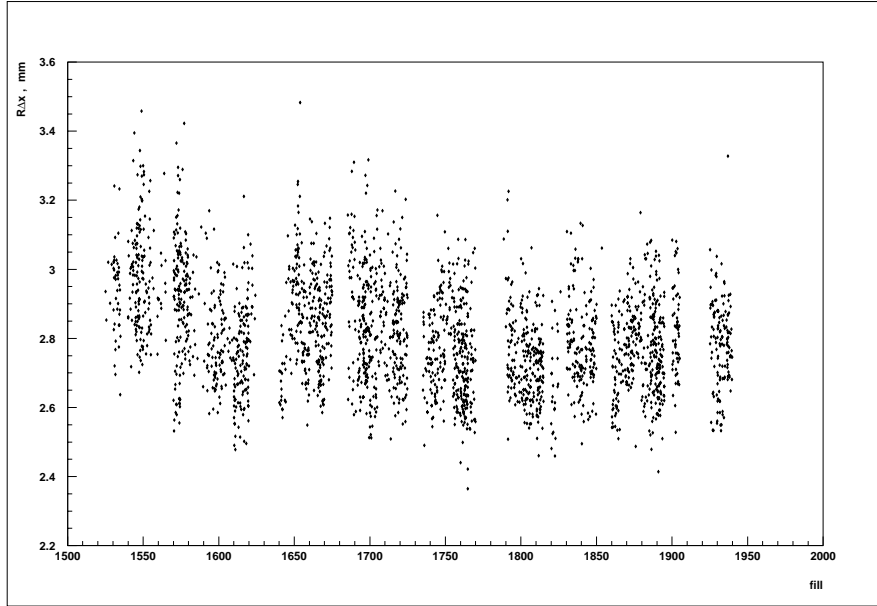
Figure 41: *Variation of $R\Delta x$ during 1993.*

The variations of the acollinearity in the (y,z) plane are shown in fig. 42. The values
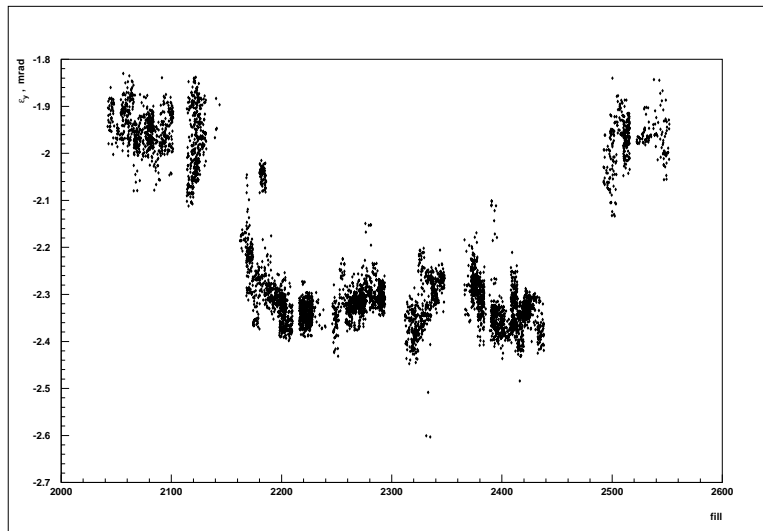
Figure 42: *Variation of ϵ_y during 1994.*

are negative and greater (in absolute value) than those of ϵ_x by about 1 mrad. In period 1, ϵ_y varied between -2.10 mrad and -1.80 mrad. In period 2, it covered the interval from -2.45 mrad to -2.10 mrad whereas the values of period 3 are from -2.10 mrad to -1.80 mrad. The 400 μrad steps between 1994 periods were not observed in 1993 data, where ϵ_y had a rather stable mean value of -0.3 mrad (fig. 43). As we saw in the beginning of
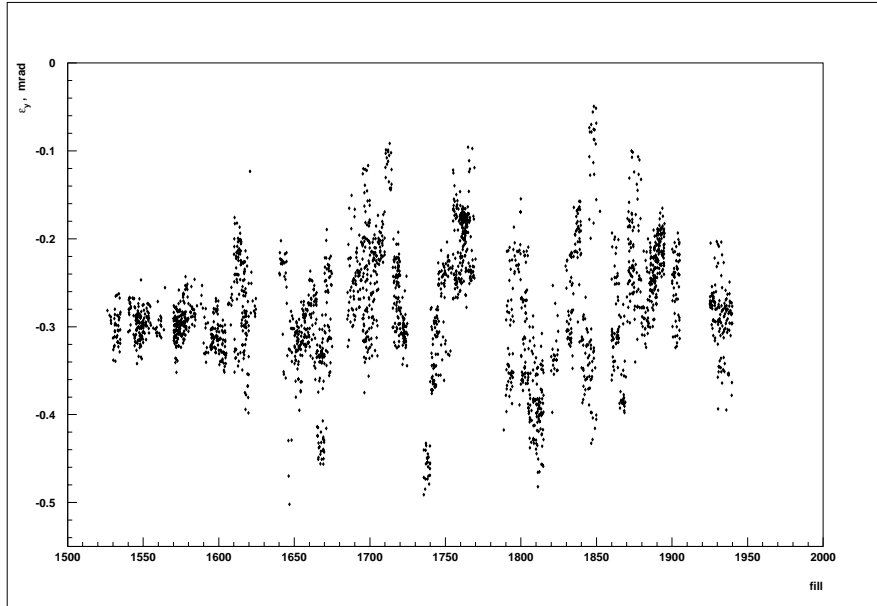
Figure 43: *Variation of ϵ_y during 1993.*

this section, the mean tilt in the (x,z) plane is connected to the asymmetry. We plot the variations of the asymmetry in fig. 44. According to eq. (31), the variations of θ_x are
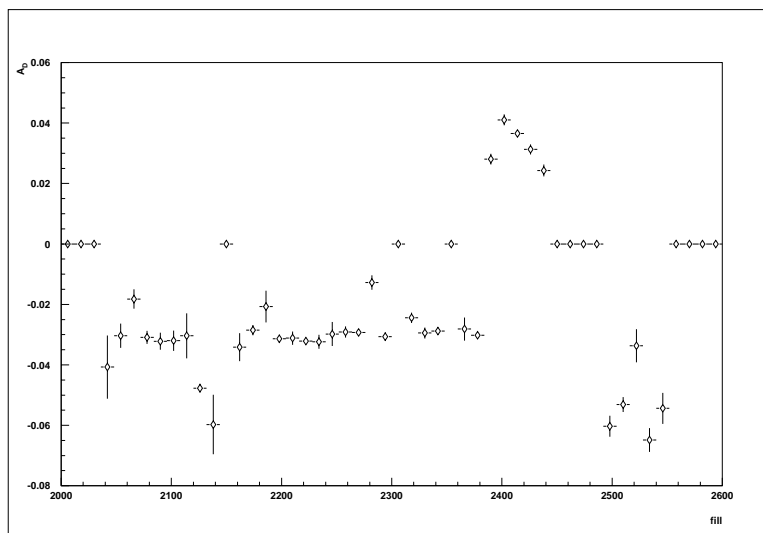
Figure 44: *Variation of the asymmetry during 1994.*

expected to be the same multiplied by the factor of 1.75. Fig. 45 and 46 suggest that θ_x varied in very similar ways during 1993 and 1994.
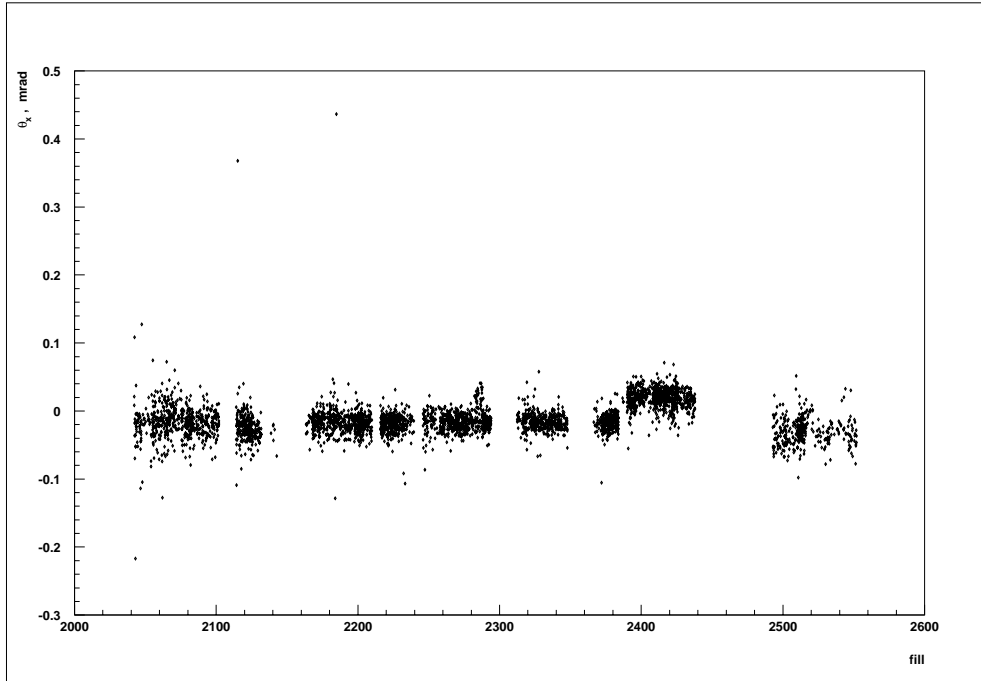
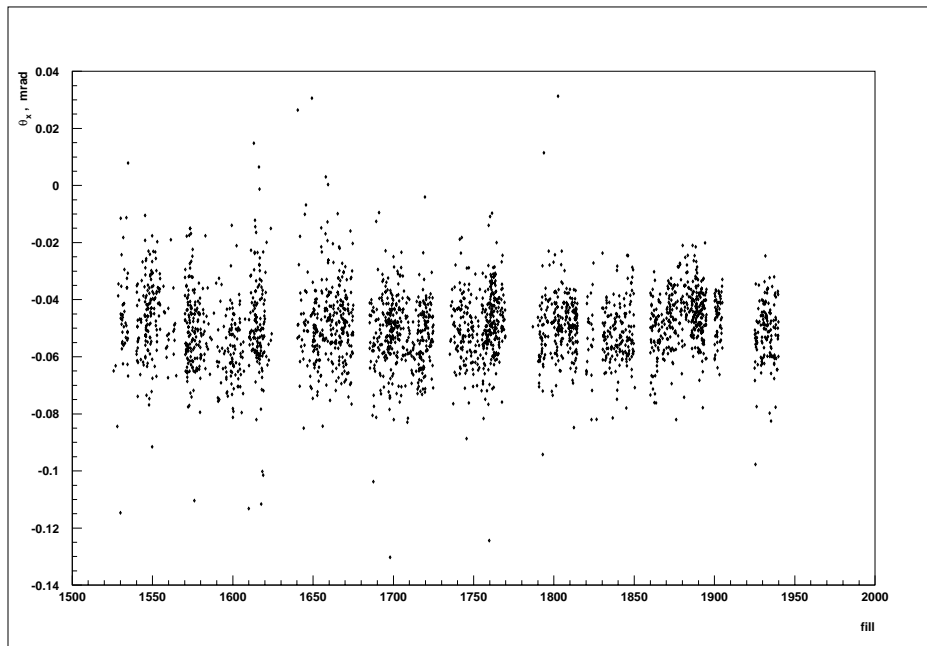Figure 45: *Variation of θ_x during 1994.*

Figure 46: *Variation of θ_x during 1993.*

Lastly, we plot the variation of the mean tilt in the (y,z) plane in fig. 47. We observe that in all periods, it varied from -0.8 mrad to -0.2 mrad. There is an increase of 50 μrad at the end of period 2 and a step of 100 μrad (decrease) from period 2 to period 3. Fig. 48 shows the variations of θ_y during 1993. We observe that it varied from -0.4 mrad to 0.3 mrad, the values of periods 1 and 2 being mostly positive.
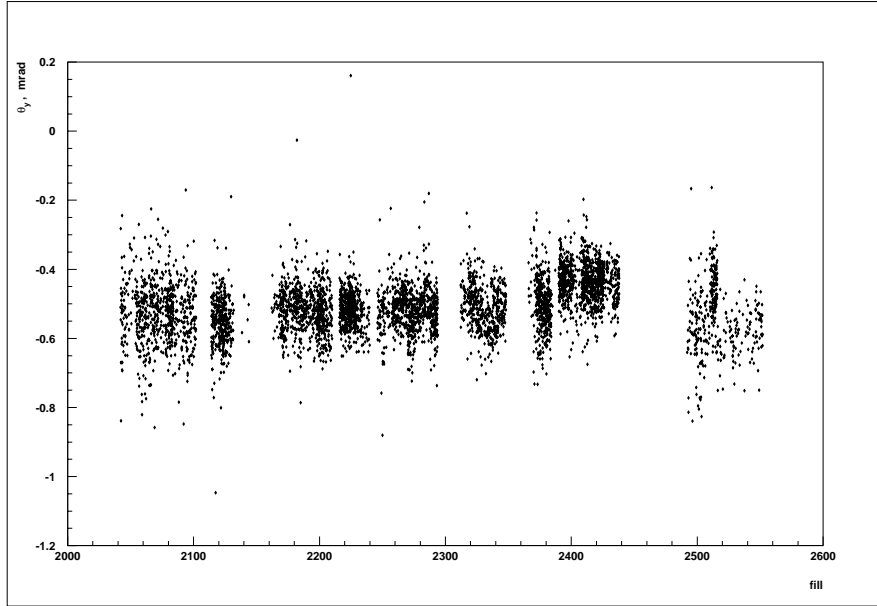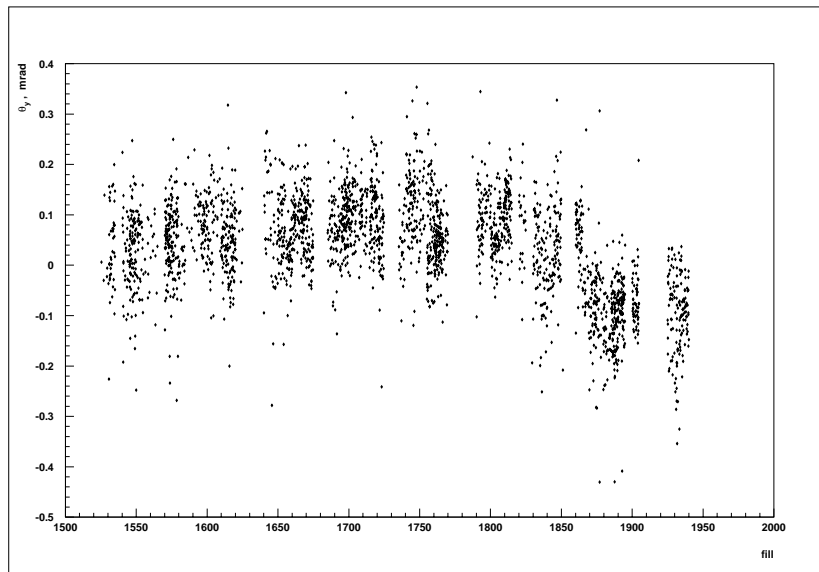

Figure 47: *Variation of θy during 1994.*

Figure 48: *Variation of θy during 1993.*

5   Conclusions

The position of the VSAT allows for high accuracy measurements of LEP beam parameters such as the asymmetry, acollinearity and tilt as well as for interaction point estimations. The comparison with the Micro Vertex estimation of x beamspot shows that the VSAT measurement is significantly shifted by the presence of the acollinearity in the (x,z) plane, otherwise both measurements show the same features. However, the comparison of the VSAT results for the y beamspot with the corresponding measure of the Micro Vertex detector shows that the acollinearity effect is much more significant in the (y,z) plane. As a consequence, the VSAT is not reliable for y beamspot estimations. The comparison with the TPC measurement of z beamspot shows a very good agreement.

Acknowledgements

References

[1] A. Håkansson, *Luminosity measurement at LEP using the Very Small Angle Tagger of DELPHI*, LUNFD6/(NFFL-7077)1993

[2] Almehed et al., *A silicon tungsten electromagnetic calorimeter for LEP*, Nucl. Instr. Meth. A305 1991

[3] Almehed et al. *High precision relative luminosity measurement with a Very Small Angle Tagger (VSAT) in DELPHI*, DELPHI 92-77 PHYS 188

[4] Almehed et al. *Beam parameter monitoring and interaction point measurement in DELPHI with the VSAT*, DELPHI 94-144 PHYS 453

[5] G. Rinaudo, private communication

[6] G. Rinaudo, private communication